COMMUNICATIONS IN COMPUTATIONAL PHYSICS
Vol. 4, No. 2, pp. 405-432

Commun. Comput. Phys.
August 2008

Splitting Finite Difference Methods on Staggered Grids for the Three-Dimensional Time-Dependent Maxwell Equations

Liping Gao[1], Bo Zhang[2,*] and Dong Liang[3]

[1] *School of Mathematical Sciences, Shandong Normal University, Jinan 250014, China.*
[2] *Institute of Applied Mathematics, Chinese Academy of Sciences, Beijing 100080, China.*
[3] *Department of Mathematics and Statistics, York University, 4700 Keele Street, Toronto, Ontario M3J 1P3, Canada.*

Received 22 July 2007; Accepted (in revised version) 5 January 2008

Communicated by Song Jiang

Available online 27 March 2008

Abstract. In this paper, we study splitting numerical methods for the three-dimensional Maxwell equations in the time domain. We propose a new kind of splitting finite-difference time-domain schemes on a staggered grid, which consists of only two stages for each time step. It is proved by the energy method that the splitting scheme is unconditionally stable and convergent for problems with perfectly conducting boundary conditions. Both numerical dispersion analysis and numerical experiments are also presented to illustrate the efficiency of the proposed schemes.

AMS subject classifications: 65N10, 65N15

Key words: Splitting scheme, alternating direction implicit method, finite-difference time-domain method, stability, convergence, Maxwell's equations, perfectly conducting boundary.

1 Introduction

In this paper we consider splitting finite difference methods for the three-dimensional Maxwell equations

$$\frac{\partial E_x}{\partial t}=\frac{1}{\varepsilon}\left(\frac{\partial H_z}{\partial y}-\frac{\partial H_y}{\partial z}-\sigma E_x\right), \tag{1.1}$$

*Corresponding author. *Email addresses:* `lipinggao68@gmail.com` (L. Gao), `b.zhang@amt.ac.cn` (B. Zhang), `dliang@mathstat.yorku.ca` (D. Liang)

$$\frac{\partial E_y}{\partial t}=\frac{1}{\varepsilon}\left(\frac{\partial H_x}{\partial z}-\frac{\partial H_z}{\partial x}-\sigma E_y\right), \tag{1.2}$$

$$\frac{\partial E_z}{\partial t}=\frac{1}{\varepsilon}\left(\frac{\partial H_y}{\partial x}-\frac{\partial H_x}{\partial y}-\sigma E_z\right), \tag{1.3}$$

$$\frac{\partial H_x}{\partial t}=\frac{1}{\mu}\left(\frac{\partial E_y}{\partial z}-\frac{\partial E_z}{\partial y}-\sigma^* H_x\right), \tag{1.4}$$

$$\frac{\partial H_y}{\partial t}=\frac{1}{\mu}\left(\frac{\partial E_z}{\partial x}-\frac{\partial E_x}{\partial z}-\sigma^* H_y\right), \tag{1.5}$$

$$\frac{\partial H_z}{\partial t}=\frac{1}{\mu}\left(\frac{\partial E_x}{\partial y}-\frac{\partial E_y}{\partial x}-\sigma^* H_z\right) \tag{1.6}$$

in a lossy medium with electric permittivity ε, magnetic permeability μ, electric conductivity σ and the equivalent magnetic loss rate σ^*, where $\mathbf{E}=(E_x,E_y,E_z)$ and $\mathbf{H}=(H_x,H_y,H_z)$ denote the electric and magnetic fields. If these fields (multiplied with ε and μ respectively) start out divergence free, they will remain so during wave propagation. Physically this is a consequence of the relations $div(\varepsilon\mathbf{E})=\rho$ (where ρ is the local charge density), and $div(\mu\mathbf{H})=0$. Their invariance in time is also a consequence of the Maxwell equations (1.1)-(1.6) and need therefore not be imposed separately.

The numerical approximation of Maxwell's equations has emerged recently as a crucial enabling technology for radio-frequency, microwave, integrated optical circuits, antennas, and wireless engineering [1–3, 13–15, 19, 24]. The finite-difference time-domain (FDTD) method, first introduced by Yee [26] (also called Yee's scheme) and extensively utilized and refined by Taflove and others [24], has been the most widely used numerical algorithm in computational electromagnetics in the time domain over the past few decades, due to its simplicity, robustness, and low cost per grid point [24]. Yee's scheme employs a fully staggered space-time grid and is explicit with a second-order convergence rate in both time and space. The stability and convergence analysis were carried out for Yee's scheme in [20, 22] using the energy method.

However, Yee's scheme is only conditionally stable so that the time step and the spatial step sizes $\Delta t, \Delta x, \Delta y$ and Δz must satisfy the Courant-Friedrichs-Lewy (CFL) stability condition

$$\Delta t \le \frac{1}{c}\left[\frac{1}{\Delta x^2}+\frac{1}{\Delta y^2}+\frac{1}{\Delta z^2}\right]^{-1/2}$$

in the three-dimensional case, where $c=1/\sqrt{\epsilon\mu}$ is the wave velocity. If the time step is not within the bound, the FDTD scheme will become numerically unstable. Thus, the computation of the three-dimensional Maxwell equations by Yee's scheme will become extremely difficult when the spatial discretization step sizes become very small. To overcome this difficulty, an unconditionally stable alternating direction implicit (ADI) FDTD scheme was first proposed in [27] and [21] for the three-dimensional Maxwell equations with an isotropic medium (see also [24]). This ADI-FDTD scheme consists of only two stages for each time step, which is different from the traditional ADI technique introduced in [5, 23] for the three-dimensional case (see also [4, 6, 7]). A detailed dispersion analysis of this ADI-FDTD scheme was conducted in [9,27,28]. A rigorous error estimate of this ADI-FDTD scheme was derived in [10] in the case of perfectly conducting boundary conditions. It should be remarked that this ADI-FDTD scheme has been studied by many authors recently (see, e.g., [8, 12, 17]).

Recently, in [11], we proposed a new kind of splitting finite-difference time-domain methods on a staggered grid for the Maxwell equations in two dimensions, which consists of only two stages for each time step and is very simple in computation. The splitting schemes were proved to be unconditionally stable and convergent in [11] for the problems with perfectly conducting boundary conditions, employing the discrete energy method. Numerical dispersion analysis and numerical experiments including a scattering problem with PML boundary conditions were also presented in [11] to show the efficient performance of the splitting schemes.

In this paper, we extend the effective splitting methods proposed in [11] for the two-dimensional Maxwell equations to the three-dimensional case. We propose a splitting finite-difference time-domain (S-FDTD) scheme on a staggered grid for the three-dimensional Maxwell equations, which consists of only two stages for each time step. By the energy method we prove that the S-FDTD scheme is unconditionally stable and convergent with first-order in time and second-order in space in the case of perfectly conducting boundary conditions. To improve the accuracy in time of the S-FDTD scheme we propose an improved splitting scheme by reducing the perturbation error of the S-FDTD scheme, which is called IS-FDTD and is of second-order in both time and space. This technique was used in [7] to improve the accuracy of ADI methods for parabolic equations. A detailed numerical dispersion analysis is carried out for the two schemes in the case of an unbounded homogeneous lossless medium. The analysis shows that the two schemes are unconditionally stable with S-FDTD being dissipative and IS-FDTD being non-dissipative and that the dispersion error of IS-FDTD is much smaller than that of S-FDTD.

In the special case with $\sigma=\sigma^*=0$, it is proved that the improved splitting scheme IS-FDTD is equivalent to the ADI-FDTD scheme proposed in [27]. However, the implementation of the ADI-FDTD scheme and the improved splitting scheme are different, so their performance is different in practical computation. In fact, the numerical experiments in Section 5 show that the improved splitting scheme, IS-FDTD, is more accurate than the ADI-FDTD scheme though IS-FDTD uses about 16.7% more CPU time than ADI-FDTD does. Further, the numerical results confirm the theoretical results that the convergence rate in time of the S-FDTD scheme is of first-order and that of the IS-FDTD and ADI-FDTD schemes is of second-order.

The remaining part of the paper is organized as follows. In Section 2, the splitting scheme S-FDTD is introduced for the general three-dimensional Maxwell equations. An improved splitting scheme (IS-FDTD) is also proposed by reducing the perturbation error in time of the S-FDTD scheme, which is equivalent to a second order perturbation of the

Crank-Nicolson (CN) scheme for the Maxwell equations. In Section 3, the unconditional stability and error estimates of the splitting scheme, S-FDTD, are established rigorously in the case of perfectly conducting boundary conditions. Section 4 is devoted to the numerical dispersion analysis of the two schemes. Numerical experiments are presented in Section 5.

2 The splitting FDTD Schemes

In this paper we consider the bounded domain problem where the medium occupies the cubic region $\Omega=[0,a]\times[0,b]\times[0,c]$ surrounded by perfect conductors, so the perfectly conducting boundary condition is satisfied:

$$\vec{\nu}\times\mathbf{E}=0 \text{ on } (0,T]\times\partial\Omega, \tag{2.1}$$

where $\partial\Omega$ denotes the boundary of Ω and $T>0$ is the terminal time. We also assume the initial conditions

$$\mathbf{E}(0,x,y,z)=\mathbf{E}_0(x,y,z) \qquad \text{and} \qquad \mathbf{H}(0,x,y,z)=\mathbf{H}_0(x,y,z). \tag{2.2}$$

It is well known that, for suitably smooth data, the problem (1.1)-(1.6) with (2.1)-(2.2) has a unique solution for all time [18]. We will assume throughout this paper that the solution of the Maxwell system has the following regularity property:

$$\mathbf{E}\in C([(0,T];[C^3(\bar{\Omega})]^3)\cap C^1([0,T];[C^1(\bar{\Omega})]^3)\cap C^2([0,T];[C(\bar{\Omega})]^3), \tag{2.3}$$
$$\mathbf{H}\in C([(0,T];[C^3(\bar{\Omega})]^3)\cap C^1([0,T];[C^1(\bar{\Omega})]^3)\cap C^2([0,T];[C(\bar{\Omega})]^3). \tag{2.4}$$

For simplicity, we only consider the constant coefficient case. The method presented here can be easily extended to the case of variable coefficients. Remarks will be made to indicate the necessary changes for the case of variable coefficients when needed.

Remark 2.1. From the Maxwell equations (1.1)-(1.6) and the boundary condition (2.1) the boundary values of $\mathbf{H}$ can be derived. In fact, from (1.4)-(1.6) and (2.1) it follows that

$$\vec{\nu}\cdot\frac{\partial\mathbf{H}}{\partial t}=-\frac{1}{\mu}(\vec{\nu}\cdot(\nabla\times\mathbf{E})+\sigma^*(\vec{\nu}\cdot\mathbf{H}))=-\frac{\sigma^*}{\mu}\vec{\nu}\cdot\mathbf{H}. \tag{2.5}$$

Since, by (2.1) and (2.2), $\vec{\nu}\times\mathbf{E}_0=0$, then we have $\vec{\nu}\cdot\mathbf{H}_0=0$ (see [16]). This together with (2.5) implies that

$$\vec{\nu}\cdot\mathbf{H}_0=0 \text{ on } (0,T]\times\partial\Omega. \tag{2.6}$$

To derive the splitting FDTD schemes for Maxwell's equations (1.1)-(1.6), we need some notations. Introduce first the following mesh on Ω:

$$\begin{aligned}\bar{\Omega}^h=\{(x_i,y_j,z_k)|x_i=i\Delta x, y_j=j\Delta y, z_k=k\Delta z,\ i=0,1\cdots,I, j=0,1,\cdots,J,\\ k=0,1,\cdots,K, x_0=y_0=z_0=0, x_I=a, y_J=b, z_K=c\},\end{aligned}$$

where Δx, Δy and Δz are the mesh sizes along the x, y and z directions, respectively. For a positive integer N let $\Delta t = T/N$ be the time step and let $t^n = n\Delta t$ with $n = 0,1,\cdots,N$. Set

$$x_{i+\frac{1}{2}} = x_i + \frac{1}{2}\Delta x,\ y_{j+\frac{1}{2}} = y_j + \frac{1}{2}\Delta y,\ z_{k+\frac{1}{2}} = z_k + \frac{1}{2}\Delta z,\ t^{n+\frac{1}{2}} = t^n + \frac{1}{2}\Delta t,$$

and for a function $F(t,x,y,z)$ define

$$\begin{aligned}
&F^m_{\alpha,\beta,\gamma} = F(m\Delta t,\alpha\Delta x,\beta\Delta y,\gamma\Delta z), &&\delta_x F^m_{\alpha,\beta,\gamma} = \frac{F^m_{\alpha+\frac{1}{2},\beta,\gamma} - F^m_{\alpha-\frac{1}{2},\beta,\gamma}}{\Delta x},\\
&\delta_y F^m_{\alpha,\beta,\gamma} = \frac{F^m_{\alpha,\beta+\frac{1}{2},\gamma} - F^m_{\alpha,\beta-\frac{1}{2},\gamma}}{\Delta y}, &&\delta_z F^m_{\alpha,\beta,\gamma} = \frac{F^m_{\alpha,\beta,\gamma+\frac{1}{2}} - F^m_{\alpha,\beta,\gamma-\frac{1}{2}}}{\Delta z},\\
&\delta_t F^m_{\alpha,\beta,\gamma} = \frac{F^{m+\frac{1}{2}}_{\alpha,\beta,\gamma} - F^{m-\frac{1}{2}}_{\alpha,\beta,\gamma}}{\Delta t}, &&\bar{\delta}_t F^m_{\alpha,\beta,\gamma} = \frac{F^{m+\frac{1}{2}}_{\alpha,\beta,\gamma} + F^{m-\frac{1}{2}}_{\alpha,\beta,\gamma}}{2}.
\end{aligned}$$

Denote by $E^m_v\big|_{\alpha,\beta,\gamma}$ and $H^m_v\big|_{\alpha,\beta,\gamma}$ the approximation of the electric field $E_v(t^m,x_\alpha,y_\beta,y_\gamma)$ and the magnetic field $H_v(t^m,x_\alpha,y_\beta,z_\gamma)$, respectively, with $v = x,y,z$. Then the splitting FDTD scheme for (1.1)-(1.6) can be written in two stages as follows:
Stage 1:

$$\frac{E^{n+\frac{1}{2}}_{x_{i+\frac{1}{2},j,k}} - E^n_{x_{i+\frac{1}{2},j,k}}}{\Delta t} = \frac{1}{\varepsilon}\delta_y \widetilde{H}^{n+\frac{1}{2}}_{z_{i+\frac{1}{2},j,k}} - \frac{\sigma}{\varepsilon}\widetilde{E}^{n+\frac{1}{2}}_{x_{i+\frac{1}{2},j,k}}, \tag{2.7}$$

$$\frac{E^{n+\frac{1}{2}}_{y_{i,j+\frac{1}{2},k}} - E^n_{y_{i,j+\frac{1}{2},k}}}{\Delta t} = \frac{1}{\varepsilon}\delta_z \widetilde{H}^{n+\frac{1}{2}}_{x_{i,j+\frac{1}{2},k}} - \frac{\sigma}{\varepsilon}\widetilde{E}^{n+\frac{1}{2}}_{y_{i,j+\frac{1}{2},k}}, \tag{2.8}$$

$$\frac{E^{n+\frac{1}{2}}_{z_{i,j,k+\frac{1}{2}}} - E^n_{z_{i,j,k+\frac{1}{2}}}}{\Delta t} = \frac{1}{\varepsilon}\delta_x \widetilde{H}^{n+\frac{1}{2}}_{y_{i,j,k+\frac{1}{2}}} - \frac{\sigma}{\varepsilon}\widetilde{E}^{n+\frac{1}{2}}_{z_{i,j,k+\frac{1}{2}}}, \tag{2.9}$$

$$\frac{H^{n+\frac{1}{2}}_{x_{i,j+\frac{1}{2},k+\frac{1}{2}}} - H^n_{x_{i,j+\frac{1}{2},k+\frac{1}{2}}}}{\Delta t} = \frac{1}{\mu}\delta_z \widetilde{E}^{n+\frac{1}{2}}_{y_{i,j+\frac{1}{2},k+\frac{1}{2}}} - \frac{\sigma^*}{\mu}\widetilde{H}^{n+\frac{1}{2}}_{x_{i,j+\frac{1}{2},k+\frac{1}{2}}}, \tag{2.10}$$

$$\frac{H^{n+\frac{1}{2}}_{y_{i+\frac{1}{2},j,k+\frac{1}{2}}} - H^n_{y_{i+\frac{1}{2},j,k+\frac{1}{2}}}}{\Delta t} = \frac{1}{\mu}\delta_x \widetilde{E}^{n+\frac{1}{2}}_{z_{i+\frac{1}{2},j,k+\frac{1}{2}}} - \frac{\sigma^*}{\mu}\widetilde{H}^{n+\frac{1}{2}}_{y_{i+\frac{1}{2},j,k+\frac{1}{2}}}, \tag{2.11}$$

$$\frac{H^{n+\frac{1}{2}}_{z_{i+\frac{1}{2},j+\frac{1}{2},k}} - H^n_{z_{i+\frac{1}{2},j+\frac{1}{2},k}}}{\Delta t} = \frac{1}{\mu}\delta_y \widetilde{E}^{n+\frac{1}{2}}_{x_{i+\frac{1}{2},j+\frac{1}{2},k}} - \frac{\sigma^*}{\mu}\widetilde{H}^{n+\frac{1}{2}}_{z_{i+\frac{1}{2},j+\frac{1}{2},k}}, \tag{2.12}$$

where the average values are defined, e.g.,

$$\widetilde{H}^{n+\frac{1}{2}}_{z_{i+\frac{1}{2},j,k}} = \frac{1}{2}\left(H^{n+\frac{1}{2}}_{z_{i+\frac{1}{2},j,k}} + H^n_{z_{i+\frac{1}{2},j,k}}\right), \quad \widetilde{E}^{n+\frac{1}{2}}_{x_{i+\frac{1}{2},j+\frac{1}{2},k}} = \frac{1}{2}\left(E^{n+\frac{1}{2}}_{x_{i+\frac{1}{2},j+\frac{1}{2},k}} + E^n_{x_{i+\frac{1}{2},j+\frac{1}{2},k}}\right). \tag{2.13}$$

Stage 2:

$$\frac{E^{n+1}_{x_{i+\frac{1}{2},j,k}}-E^{n+\frac{1}{2}}_{x_{i+\frac{1}{2},j,k}}}{\Delta t}=-\frac{1}{\varepsilon}\delta_z\overline{H}^{n+\frac{1}{2}}_{y_{i+\frac{1}{2},j,k}},\quad \frac{E^{n+1}_{y_{i,j+\frac{1}{2},k}}-E^{n+\frac{1}{2}}_{y_{i,j+\frac{1}{2},k}}}{\Delta t}=-\frac{1}{\varepsilon}\delta_x\overline{H}^{n+\frac{1}{2}}_{z_{i,j+\frac{1}{2},k}}, \tag{2.14}$$

$$\frac{E^{n+1}_{z_{i,j,k+\frac{1}{2}}}-E^{n+\frac{1}{2}}_{z_{i,j,k+\frac{1}{2}}}}{\Delta t}=-\frac{1}{\varepsilon}\delta_y\overline{H}^{n+\frac{1}{2}}_{x_{i,j,k+\frac{1}{2}}}, \tag{2.15}$$

$$\frac{H^{n+1}_{x_{i,j+\frac{1}{2},k+\frac{1}{2}}}-H^{n+\frac{1}{2}}_{x_{i,j+\frac{1}{2},k+\frac{1}{2}}}}{\Delta t}=-\frac{1}{\mu}\delta_y\overline{E}^{n+\frac{1}{2}}_{z_{i,j+\frac{1}{2},k+\frac{1}{2}}}, \tag{2.16}$$

$$\frac{H^{n+1}_{y_{i+\frac{1}{2},j,k+\frac{1}{2}}}-H^{n+\frac{1}{2}}_{y_{i+\frac{1}{2},j,k+\frac{1}{2}}}}{\Delta t}=-\frac{1}{\mu}\delta_z\overline{E}^{n+\frac{1}{2}}_{x_{i+\frac{1}{2},j,k+\frac{1}{2}}}, \tag{2.17}$$

$$\frac{H^{n+1}_{z_{i+\frac{1}{2},j+\frac{1}{2},k}}-H^{n+\frac{1}{2}}_{z_{i+\frac{1}{2},j+\frac{1}{2},k}}}{\Delta t}=-\frac{1}{\mu}\delta_x\overline{E}^{n+\frac{1}{2}}_{y_{i+\frac{1}{2},j+\frac{1}{2},k}}, \tag{2.18}$$

where the average value is defined in the conventional way, e.g.,

$$\overline{H}^{n+\frac{1}{2}}_{z_{i+\frac{1}{2},j,k}}=\frac{1}{2}\left(H^{n+1}_{z_{i+\frac{1}{2},j,k}}+H^{n}_{z_{i+\frac{1}{2},j,k}}\right),\quad \overline{E}^{n+\frac{1}{2}}_{y_{i+\frac{1}{2},j+\frac{1}{2},k}}=\frac{1}{2}\left(E^{n+1}_{y_{i+\frac{1}{2},j+\frac{1}{2},k}}+E^{n}_{y_{i+\frac{1}{2},j+\frac{1}{2},k}}\right). \tag{2.19}$$

By the definition of the cross product of vectors the boundary condition (2.1) is satisfied by letting

$$E^m_{x_{i+\frac{1}{2},0,k}}=E^m_{x_{i+\frac{1}{2},J,k}}=E^m_{x_{i+\frac{1}{2},j,0}}=E^m_{x_{i+\frac{1}{2},j,K}}=0, \tag{2.20}$$

$$E^m_{y_{0,j+\frac{1}{2},k}}=E^m_{y_{I,j+\frac{1}{2},k}}=E^m_{y_{i,j+\frac{1}{2},0}}=E^m_{y_{i,j+\frac{1}{2},K}}=0, \tag{2.21}$$

$$E^m_{z_{0,j,k+\frac{1}{2}}}=E^m_{z_{I,j,k+\frac{1}{2}}}=E^m_{z_{i,0,k+\frac{1}{2}}}=E^m_{z_{i,J,k+\frac{1}{2}}}=0, \tag{2.22}$$

with $m=n$. The case with $m=n+\frac{1}{2}$ is also true by using the scheme (2.7)-(2.18) in conjunction with (2.1) and (2.6). Finally, the initial values $\mathbf{E}^0_{\alpha,\beta,\gamma}$ and $\mathbf{H}^0_{\alpha,\beta,\gamma}$ are obtained by imposing the initial condition (2.2) at $t=0$, that is,

$$\mathbf{E}^0_{\alpha,\beta,\gamma}=\mathbf{E}_0(\alpha\Delta x,\beta\Delta y,\gamma\Delta z),\qquad \mathbf{H}^0_{\alpha,\beta,\gamma}=\mathbf{H}_0(\alpha\Delta x,\beta\Delta y,\gamma\Delta z). \tag{2.23}$$

The above splitting scheme (2.7)-(2.18) (called S-FDTD) is based on splitting of Maxwell's equations and its symmetric structure and consists of only two stages for each time step $[t^n,t^{n+1}]$. At each stage the splitting scheme S-FDTD can be solved effectively by first solving three tridiagonal systems of equations for, say, the three components E_x,E_y,E_z of the electric field and then computing H_x,H_y,H_z explicitly. For example, using

(2.12) to eliminate $H_{z_{i+\frac{1}{2},j+\frac{1}{2},k}}^{n+\frac{1}{2}}$ and $H_{z_{i+\frac{1}{2},j-\frac{1}{2},k}}^{n+\frac{1}{2}}$ in (2.7) gives

$$
\begin{aligned}
&-\frac{(\Delta t)^2}{4(\Delta y)^2}E_{x_{i+\frac{1}{2},j-1,k}}^{n+\frac{1}{2}}+\left[\mu^+\varepsilon^++\frac{(\Delta t)^2}{2(\Delta y)^2}\right]E_{x_{i+\frac{1}{2},j,k}}^{n+\frac{1}{2}}-\frac{(\Delta t)^2}{4(\Delta y)^2}E_{x_{i+\frac{1}{2},j+1,k}}^{n+\frac{1}{2}}\\
=&\,\mu^+\varepsilon^-E_{x_{i+\frac{1}{2},j,k}}^{n}+\Delta t\mu^-\delta_yH_{z_{i+\frac{1}{2},j,k}}^{n}+\frac{(\Delta t)^2}{4}\delta_y\delta_yE_{x_{i+\frac{1}{2},j,k}}^{n},
\end{aligned}
\tag{2.24}
$$

where

$$
\varepsilon^+=\varepsilon+\frac{1}{2}\sigma\Delta t,\quad \varepsilon^-=\varepsilon-\frac{1}{2}\sigma\Delta t,\quad \mu^+=\mu+\frac{1}{2}\sigma^*\Delta t,\quad \mu^-=\mu-\frac{1}{2}\sigma^*\Delta t.
$$

Eq. (2.24) is tridiagonal for $E_x^{n+1/2}$ with all the field components on the right hand side being known from the previous time step and can be solved efficiently for the values of $E_x^{n+1/2}$ at the grid points

$$
\{((i+1/2)\Delta x, j\Delta y, k\Delta z)\,|\, j=0,1,\cdots,J\}.
$$

This can be seen as solving a one-dimensional problem in the y direction. Note that the coefficient matrix of the tridiagonal system (2.24) does not change with the time level n. $H_z^{n+1/2}$ then follows explicitly from the equation

$$
H_{z_{i+\frac{1}{2},j+\frac{1}{2},k}}^{n+\frac{1}{2}}=\frac{\mu^-}{\mu^+}H_{z_{i+\frac{1}{2},j+\frac{1}{2},k}}^{n}+\frac{\Delta t}{2\mu^+}\delta_y\left(E_{x_{i+\frac{1}{2},j+\frac{1}{2},k}}^{n+\frac{1}{2}}+E_{x_{i+\frac{1}{2},j+\frac{1}{2},k}}^{n}\right).
$$

Similarly, we can obtain and solve the tridiagonal systems for E_y, E_z, and H_y, H_z then follow explicitly.

Remark 2.2. The S-FDTD scheme is different from the conventional ADI procedure in [4–6, 23], where the alternations in the computation directions are made with respect to the three spatial coordinate directions so, in the 3-D case, the computation is broken down into three stages for each time step.

Remark 2.3. The S-FDTD scheme is also different from the ADI-FDTD scheme proposed in [27] and [21]. From (2.7)-(2.18) it is found that the values of the electric and magnetic fields at the intermediate time levels are not the real values of the fields at the time levels.

The truncation error of the S-FDTD scheme is of first order in time, as seen from the detailed analysis in the next section. In order to improve the accuracy of the S-FDTD scheme, we give an improved scheme by reducing the perturbation error of the S-FDTD scheme. The improved scheme (called IS-FDTD) becomes a second-order perturbation to the CN scheme for the Maxwell equations.

The IS-FDTD scheme is defined as follows:
Stage 1:

$$\frac{E^{n+\frac{1}{2}}_{x_{i+\frac{1}{2},j,k}}-E^{n}_{x_{i+\frac{1}{2},j,k}}}{\Delta t}=\frac{1}{\varepsilon}\delta_y\widetilde{H}^{n+\frac{1}{2}}_{z_{i+\frac{1}{2},j,k}}-\frac{\sigma}{\varepsilon}\widetilde{E}^{n+\frac{1}{2}}_{x_{i+\frac{1}{2},j,k}}-\frac{\Delta t}{2\mu\varepsilon}\delta_y\delta_x E^{n}_{y_{i+\frac{1}{2},j,k}}+\frac{\sigma\Delta t}{2\varepsilon^2}\delta_z H^{n}_{y_{i+\frac{1}{2},j,k}},\tag{2.25}$$

$$\frac{E^{n+\frac{1}{2}}_{y_{i,j+\frac{1}{2},k}}-E^{n}_{y_{i,j+\frac{1}{2},k}}}{\Delta t}=\frac{1}{\varepsilon}\delta_z\widetilde{H}^{n+\frac{1}{2}}_{x_{i,j+\frac{1}{2},k}}-\frac{\sigma}{\varepsilon}\widetilde{E}^{n+\frac{1}{2}}_{y_{i,j+\frac{1}{2},k}}-\frac{\Delta t}{2\mu\varepsilon}\delta_z\delta_y E^{n}_{z_{i,j+\frac{1}{2},k}}+\frac{\sigma\Delta t}{2\varepsilon^2}\delta_x H^{n}_{z_{i,j+\frac{1}{2},k}},\tag{2.26}$$

$$\frac{E^{n+\frac{1}{2}}_{z_{i,j,k+\frac{1}{2}}}-E^{n}_{z_{i,j,k+\frac{1}{2}}}}{\Delta t}=\frac{1}{\varepsilon}\delta_x\widetilde{H}^{n+\frac{1}{2}}_{y_{i,j,k+\frac{1}{2}}}-\frac{\sigma}{\varepsilon}\widetilde{E}^{n+\frac{1}{2}}_{z_{i,j,k+\frac{1}{2}}}-\frac{\Delta t}{2\mu\varepsilon}\delta_x\delta_z E^{n}_{x_{i,j,k+\frac{1}{2}}}+\frac{\sigma\Delta t}{2\varepsilon^2}\delta_y H^{n}_{x_{i,j,k+\frac{1}{2}}},\tag{2.27}$$

$$\begin{aligned}\frac{H^{n+\frac{1}{2}}_{x_{i,j+\frac{1}{2},k+\frac{1}{2}}}-H^{n}_{x_{i,j+\frac{1}{2},k+\frac{1}{2}}}}{\Delta t}=&\frac{1}{\mu}\delta_z\widetilde{E}^{n+\frac{1}{2}}_{y_{i,j+\frac{1}{2},k+\frac{1}{2}}}-\frac{\sigma^*}{\mu}\widetilde{H}^{n+\frac{1}{2}}_{x_{i,j+\frac{1}{2},k+\frac{1}{2}}}\\&-\frac{\Delta t}{2\mu\varepsilon}\delta_z\delta_x H^{n}_{z_{i,j+\frac{1}{2},k+\frac{1}{2}}}+\frac{\sigma^*\Delta t}{2\mu^2}\delta_y E^{n}_{z_{i,j+\frac{1}{2},k+\frac{1}{2}}},\end{aligned}\tag{2.28}$$

$$\begin{aligned}\frac{H^{n+\frac{1}{2}}_{y_{i+\frac{1}{2},j,k+\frac{1}{2}}}-H^{n}_{y_{i+\frac{1}{2},j,k+\frac{1}{2}}}}{\Delta t}=&\frac{1}{\mu}\delta_x\widetilde{E}^{n+\frac{1}{2}}_{z_{i+\frac{1}{2},j,k+\frac{1}{2}}}-\frac{\sigma^*}{\mu}\widetilde{H}^{n+\frac{1}{2}}_{y_{i+\frac{1}{2},j,k+\frac{1}{2}}}\\&-\frac{\Delta t}{2\mu\varepsilon}\delta_x\delta_y H^{n}_{x_{i+\frac{1}{2},j,k+\frac{1}{2}}}+\frac{\sigma^*\Delta t}{2\mu^2}\delta_z E^{n}_{x_{i+\frac{1}{2},j,k+\frac{1}{2}}},\end{aligned}\tag{2.29}$$

$$\begin{aligned}\frac{H^{n+\frac{1}{2}}_{z_{i+\frac{1}{2},j+\frac{1}{2},k}}-H^{n}_{z_{i+\frac{1}{2},j+\frac{1}{2},k}}}{\Delta t}=&\frac{1}{\mu}\delta_y\widetilde{E}^{n+\frac{1}{2}}_{x_{i+\frac{1}{2},j+\frac{1}{2},k}}-\frac{\sigma^*}{\mu}\widetilde{H}^{n+\frac{1}{2}}_{z_{i+\frac{1}{2},j+\frac{1}{2},k}}\\&-\frac{\Delta t}{2\mu\varepsilon}\delta_y\delta_z H^{n}_{y_{i+\frac{1}{2},j+\frac{1}{2},k}}+\frac{\sigma^*\Delta t}{2\mu^2}\delta_x E^{n}_{y_{i+\frac{1}{2},j+\frac{1}{2},k}},\end{aligned}\tag{2.30}$$

where $\widetilde{H}$ and $\widetilde{E}$ are defined in (2.13).

Stage 2: Same as (2.14)-(2.18) in Stage 2 of S-FDTD.

The initial and boundary conditions for this scheme are the same as given for the S-FDTD scheme.

The IS-FDTD scheme is just a modification of the S-FDTD scheme by adding only one previous time level terms to Eqs. (2.7)-(2.12). The IS-FDTD scheme can also be solved similarly as in solving the S-FDTD scheme (see the discussion above).

Remark 2.4. The truncation error of the IS-FDTD scheme is of second order in both space and time. This can be seen from the following equivalent scheme to IS-FDTD, which can be easily obtained by eliminating the intermediate values of the fields:

$$\begin{aligned}\delta_t E_x^{n+\frac{1}{2}} =& \frac{1}{\varepsilon}\{\delta_y\bar{\delta}_t H_z^{n+\frac{1}{2}} - \delta_z\bar{\delta}_t H_y^{n+\frac{1}{2}} - \sigma\bar{\delta}_t E_x^{n+\frac{1}{2}}\} \\ &+ \frac{(\Delta t)^2}{4\mu\varepsilon}\delta_y\delta_x\delta_t E_y^{n+\frac{1}{2}} - \frac{\sigma(\Delta t)^2}{4\varepsilon^2}\delta_z\delta_t H_y^{n+\frac{1}{2}},\end{aligned} \tag{2.31}$$

$$\begin{aligned}\delta_t E_y^{n+\frac{1}{2}} =& \frac{1}{\varepsilon}\{\delta_z\bar{\delta}_t H_x^{n+\frac{1}{2}} - \delta_x\bar{\delta}_t H_z^{n+\frac{1}{2}} - \sigma\bar{\delta}_t E_y^{n+\frac{1}{2}}\} \\ &+ \frac{(\Delta t)^2}{4\mu\varepsilon}\delta_z\delta_y\delta_t E_z^{n+\frac{1}{2}} - \frac{\sigma(\Delta t)^2}{4\varepsilon^2}\delta_x\delta_t H_z^{n+\frac{1}{2}},\end{aligned} \tag{2.32}$$

$$\begin{aligned}\delta_t E_z^{n+\frac{1}{2}} =& \frac{1}{\varepsilon}\{\delta_x\bar{\delta}_t H_y^{n+\frac{1}{2}} - \delta_y\bar{\delta}_t H_x^{n+\frac{1}{2}} - \sigma\bar{\delta}_t E_z^{n+\frac{1}{2}}\} \\ &+ \frac{(\Delta t)^2}{4\mu\varepsilon}\delta_x\delta_z\delta_t E_x^{n+\frac{1}{2}} - \frac{\sigma(\Delta t)^2}{4\varepsilon^2}\delta_y\delta_t H_x^{n+\frac{1}{2}};\end{aligned} \tag{2.33}$$

similar formulas hold for H_x, H_y and H_z. The scheme (2.31)-(2.33) is the CN scheme for the Maxwell equations plus second-order perturbation terms (the last two terms in each of (2.31)-(2.33)). Thus, the improved splitting scheme IS-FDTD is equivalent to a second-order perturbation of the CN scheme for the Maxwell equations, so the local truncation error of the scheme is of second-order in both space and time. This is also confirmed by their numerical dispersion relations in Section 4 and numerical experiments in Section 5.

Remark 2.5. In the IS-FDTD scheme the values of the electric and magnetic fields at the intermediate time levels are not the real values of the fields at the time levels. Thus, the IS-FDTD scheme is in general different from the ADI-FDTD scheme proposed in [27] and [21]. In the special case with $\sigma=\sigma^*=0$, however, the equivalent form of the ADI-FDTD scheme proposed in [27] is exactly the same as (2.31)-(2.33). This means that, in this special case, the ADI-FDTD scheme and the improved splitting scheme IS-FDTD are equivalent theoretically so their numerical dispersion relations are the same. But, the implementation of the two schemes are different, so their performance will be different in practical computation. In fact, the numerical experiments in Section 5 shows that the improved splitting scheme IS-FDTD is more accurate than the ADI-FDTD scheme.

Remark 2.6. Our technique of deriving the improved splitting scheme, IS-FDTD, is based on an idea proposed in [7] for the ADI scheme of parabolic equations. The IS-FDTD scheme is different from the S-FDTD scheme only by two terms in each of the six equations at Stage 1. These added terms contain values of fields at only one time level, which is different from that in [7], where the terms added to a second-order ADI scheme for a parabolic equation contain values of the solution at two time levels. A different idea to improve the truncation error of splitting schemes is Strang's splitting: a half-step in one direction, a whole step in the other, a half-step in the first direction. However, this splitting technique is not straightforward for the S-FDTD scheme and needs further investigation.

3 Error estimates and stability analysis

In this section we establish error estimates and the unconditional stability of the splitting scheme S-FDTD by using the energy method. To this end, we define two discrete energy norms. For

$$\mathbf{V}=(V_{x_{i+\frac{1}{2},j,k}},V_{y_{i,j+\frac{1}{2},k}},V_{z_{i,j,k+\frac{1}{2}}}),\quad \mathbf{W}=(W_{x_{i,j+\frac{1}{2},k+\frac{1}{2}}},W_{y_{i+\frac{1}{2},j,k+\frac{1}{2}}},W_{z_{i+\frac{1}{2},j+\frac{1}{2},k}}),$$

define the following discrete norms:

$$\begin{aligned}\|\mathbf{V}\|_E^2&=\left[\sum_{i=0}^{I-1}\sum_{j=1}^{J-1}\sum_{k=1}^{K-1}V^2_{x_{i+\frac{1}{2},j,k}}+\sum_{i=1}^{I-1}\sum_{j=0}^{J-1}\sum_{k=1}^{K-1}V^2_{y_{i,j+\frac{1}{2},k}}+\sum_{i=1}^{I-1}\sum_{j=1}^{J-1}\sum_{k=0}^{K-1}V^2_{z_{i,j,k+\frac{1}{2}}}\right]\Delta x\Delta y\Delta z,\\ \|\mathbf{W}\|_H^2&=\left[\sum_{i=0}^{I}\sum_{j=0}^{J-1}\sum_{k=0}^{K-1}W^2_{x_{i,j+\frac{1}{2},k+\frac{1}{2}}}+\sum_{i=0}^{I-1}\sum_{j=0}^{J}\sum_{k=0}^{K-1}W^2_{y_{i+\frac{1}{2},j,k+\frac{1}{2}}}+\sum_{i=0}^{I-1}\sum_{j=0}^{J-1}\sum_{k=0}^{K}W^2_{z_{i+\frac{1}{2},j+\frac{1}{2},k}}\right]\Delta x\Delta y\Delta z.\end{aligned}$$

For

$$\mathbf{U}=(U_{x_{\alpha,\beta,\gamma}},U_{y_{\alpha,\beta,\gamma}},U_{z_{\alpha,\beta,\gamma}}),$$

define

$$\delta_1^h\mathbf{U}=(\delta_y U_{z_{\alpha,\beta,\gamma}},\delta_z U_{x_{\alpha,\beta,\gamma}},\delta_x U_{y_{\alpha,\beta,\gamma}}),\qquad \delta_2^h\mathbf{U}=(\delta_z U_{y_{\alpha,\beta,\gamma}},\delta_x U_{z_{\alpha,\beta,\gamma}},\delta_y U_{x_{\alpha,\beta,\gamma}}).$$

We then have the following result on error estimates of the splitting scheme S-FDTD.

Theorem 3.1. *Let* $\mathbf{E}$ *and* $\mathbf{H}$ *be the solution of the Maxwell equations* (1.1)-(1.6) *with the boundary condition* (2.1) *and the initial conditions* (2.2). *For* $n\ge 0$ *let*

$$\mathbf{E}^n=(E^n_{x_{i+\frac{1}{2},j,k}},E^n_{y_{i,j+\frac{1}{2},k}},E^n_{z_{i,j,k+\frac{1}{2}}}),\qquad \mathbf{H}^n=(H^n_{x_{i,j+\frac{1}{2},k+\frac{1}{2}}},H^n_{y_{i+\frac{1}{2},j,k+\frac{1}{2}}},H^n_{z_{i+\frac{1}{2},j+\frac{1}{2},k}})$$

be the solution of the S-FDTD scheme. Assume that the regularity property (2.3)-(2.4) *is true. Then, for any fixed* $T>0$, *there is constant* C *independent of* $\Delta t,\Delta x,\Delta y,\Delta z$ *such that*

$$\begin{aligned}&\max_{0\le n\le N}\left[\|\mathbf{E}(t^n)-\mathbf{E}^n\|_E+\|\mathbf{H}(t^n)-\mathbf{H}^n\|_H\right]\\ &\le C\left[\Delta t+(\Delta x)^2+(\Delta y)^2+(\Delta z)^2\right], &(3.1)\\ &\max_{0\le n\le N}\left[\|\delta_t(\mathbf{E}(t^{n+\frac{1}{2}})-\mathbf{E}^{n+\frac{1}{2}})\|_E+\|\delta_t(\mathbf{H}(t^{n+\frac{1}{2}})-\mathbf{H}^{n+\frac{1}{2}})\|_H\right]\\ &\le C\left[\Delta t+(\Delta x)^2+(\Delta y)^2+(\Delta z)^2\right]. &(3.2)\end{aligned}$$

Proof. To prove Theorem 3.1, let us define

$$\mathcal{E}^n_{w_{\alpha,\beta,\gamma}}=E_w(t^n,x_\alpha,y_\beta,z_\gamma)-E^n_{w_{\alpha,\beta,\gamma}},\quad \mathcal{H}^n_{w_{\alpha,\beta,\gamma}}=H_w(t^n,x_\alpha,y_\beta,z_\gamma)-H^n_{w_{\alpha,\beta,\gamma}}$$

for all valid choices of subscripts α,β,γ and for $w=x,y,z$. Set

$$\mathcal{E}^n=(\mathcal{E}_x^n,\mathcal{E}_y^n,\mathcal{E}_z^n),\quad \mathcal{H}^n=(\mathcal{H}_x^n,\mathcal{H}_y^n,\mathcal{H}_z^n).$$

In order to get the error equations we need to derive the following equivalent form of the S-FDTD scheme by eliminating the electric and magnetic fields at the intermediate time levels, $E^{n+\frac{1}{2}}_{u_{\alpha,\beta,\gamma}}$ and $H^{n+\frac{1}{2}}_{u_{\alpha,\beta,\gamma}}$ ($u=x,y,z$), from the splitting scheme (2.7)-(2.18):

$$\begin{aligned}\delta_t E^{n+\frac{1}{2}}_{x_{i+\frac{1}{2},j,k}} =& \frac{1}{\varepsilon}\Big\{\delta_y\bar{\delta}_t H^{n+\frac{1}{2}}_{z_{i+\frac{1}{2},j,k}}-\delta_z\bar{\delta}_t H^{n+\frac{1}{2}}_{y_{i+\frac{1}{2},j,k}}-\sigma\bar{\delta}_t E^{n+\frac{1}{2}}_{x_{i+\frac{1}{2},j,k}}\Big\}\\ &+\frac{\Delta t}{2\varepsilon}\delta_y\left[\frac{1}{\mu}\delta_x\bar{\delta}_t E^{n+\frac{1}{2}}_{y_{i+\frac{1}{2},j,k}}\right]-\frac{\sigma\Delta t}{2\varepsilon^2}\delta_z\bar{\delta}_t H^{n+\frac{1}{2}}_{y_{i+\frac{1}{2},j,k}},\end{aligned}\tag{3.3}$$

$$\begin{aligned}\delta_t E^{n+\frac{1}{2}}_{y_{i,j+\frac{1}{2},k}} =& \frac{1}{\varepsilon}\Big\{\delta_z\bar{\delta}_t H^{n+\frac{1}{2}}_{x_{i,j+\frac{1}{2},k}}-\delta_x\bar{\delta}_t H^{n+\frac{1}{2}}_{z_{i,j+\frac{1}{2},k}}-\sigma\bar{\delta}_t E^{n+\frac{1}{2}}_{y_{i,j+\frac{1}{2},k}}\Big\}\\ &+\frac{\Delta t}{2\varepsilon}\delta_z\left[\frac{1}{\mu}\delta_y\bar{\delta}_t E^{n+\frac{1}{2}}_{z_{i,j+\frac{1}{2},k}}\right]-\frac{\sigma\Delta t}{2\varepsilon^2}\delta_x\bar{\delta}_t H^{n+\frac{1}{2}}_{z_{i,j+\frac{1}{2},k}},\end{aligned}\tag{3.4}$$

$$\begin{aligned}\delta_t E^{n+\frac{1}{2}}_{z_{i,j,k+\frac{1}{2}}} =& \frac{1}{\varepsilon}\Big\{\delta_x\bar{\delta}_t H^{n+\frac{1}{2}}_{y_{i,j,k+\frac{1}{2}}}-\delta_y\bar{\delta}_t H^{n+\frac{1}{2}}_{x_{i,j,k+\frac{1}{2}}}-\sigma\bar{\delta}_t E^{n+\frac{1}{2}}_{z_{i,j,k+\frac{1}{2}}}\Big\}\\ &+\frac{\Delta t}{2\varepsilon}\delta_x\left[\frac{1}{\mu}\delta_z\bar{\delta}_t E^{n+\frac{1}{2}}_{x_{i,j,k+\frac{1}{2}}}\right]-\frac{\sigma\Delta t}{2\varepsilon^2}\delta_y\bar{\delta}_t H^{n+\frac{1}{2}}_{x_{i,j,k+\frac{1}{2}}};\end{aligned}\tag{3.5}$$

similar formulas hold for $\delta_t H^{n+\frac{1}{2}}_{x_{i,j+\frac{1}{2},k+\frac{1}{2}}}$, $\delta_t H^{n+\frac{1}{2}}_{y_{i+\frac{1}{2},j,k+\frac{1}{2}}}$ and $\delta_t H^{n+\frac{1}{2}}_{z_{i+\frac{1}{2},j+\frac{1}{2},k}}$. Then from (1.1)-(1.3) and (3.3)-(3.5) we have the following error equations:

$$\begin{aligned}&\mathcal{E}_x^{n+1}-\frac{\Delta t}{2\varepsilon}\{\delta_y\mathcal{H}_z^{n+1}-\delta_z\mathcal{H}_y^{n+1}-\sigma\mathcal{E}_x^{n+1}\}-\frac{(\Delta t)^2}{4\varepsilon}\delta_y[\frac{1}{\mu}\delta_x\mathcal{E}_y^{n+1}]+\frac{\sigma(\Delta t)^2}{4\varepsilon^2}\delta_z\mathcal{H}_y^{n+1}\\ =&\mathcal{E}_x^{n}+\frac{\Delta t}{2\varepsilon}\{\delta_y\mathcal{H}_z^{n}-\delta_z\mathcal{H}_y^{n}-\sigma\mathcal{E}_x^{n}\}+\frac{(\Delta t)^2}{4\varepsilon}\delta_y[\frac{1}{\mu}\delta_x\mathcal{E}_y^{n}]-\frac{\sigma(\Delta t)^2}{4\varepsilon^2}\delta_z\mathcal{H}_y^{n}+\Delta t{\xi_x}^{n+\frac{1}{2}},\end{aligned}\tag{3.6}$$

$$\begin{aligned}&\mathcal{E}_y^{n+1}-\frac{\Delta t}{2\varepsilon}\{\delta_z\mathcal{H}_x^{n+1}-\delta_x\mathcal{H}_z^{n+1}-\sigma\mathcal{E}_y^{n+1}\}-\frac{(\Delta t)^2}{4\varepsilon}\delta_z[\frac{1}{\mu}\delta_y\mathcal{E}_z^{n+1}]+\frac{\sigma(\Delta t)^2}{4\varepsilon^2}\delta_x\mathcal{H}_z^{n+1}\\ =&\mathcal{E}_y^{n}+\frac{\Delta t}{2\varepsilon}\{\delta_z\mathcal{H}_x^{n}-\delta_x\mathcal{H}_z^{n}-\sigma\mathcal{E}_y^{n}\}+\frac{(\Delta t)^2}{4\varepsilon}\delta_z[\frac{1}{\mu}\delta_y\mathcal{E}_z^{n}]-\frac{\sigma(\Delta t)^2}{4\varepsilon^2}\delta_x\mathcal{H}_z^{n}+\Delta t{\xi_y}^{n+\frac{1}{2}},\end{aligned}\tag{3.7}$$

$$\begin{aligned}&\mathcal{E}_z^{n+1}-\frac{\Delta t}{2\varepsilon}\{\delta_x\mathcal{H}_y^{n+1}-\delta_y\mathcal{H}_x^{n+1}-\sigma\mathcal{E}_z^{n+1}\}-\frac{(\Delta t)^2}{4\varepsilon}\delta_x[\frac{1}{\mu}\delta_z\mathcal{E}_x^{n+1}]+\frac{\sigma(\Delta t)^2}{4\varepsilon^2}\delta_y\mathcal{H}_x^{n+1}\\ =&\mathcal{E}_z^{n}+\frac{\Delta t}{2\varepsilon}\{\delta_x\mathcal{H}_y^{n}-\delta_y\mathcal{H}_x^{n}-\sigma\mathcal{E}_y^{n}\}+\frac{(\Delta t)^2}{4\varepsilon}\delta_x[\frac{1}{\mu}\delta_z\mathcal{E}_x^{n}]-\frac{\sigma(\Delta t)^2}{4\varepsilon^2}\delta_y\mathcal{H}_x^{n}+\Delta t{\xi_z}^{n+\frac{1}{2}},\end{aligned}\tag{3.8}$$

where, for simplicity, we have omitted all the subscripts since they are the same in each equation, and $\xi_u^{n+1/2}$ and $\eta_u^{n+1/2}$ with $u=x,y,z$ are the truncation errors which can be expressed by the Taylor expansion theorem. For example,

$$\begin{aligned}\xi_{x_{i+\frac{1}{2},j,k}}^{n+\frac{1}{2}}=&\Delta t\Big[\frac{\sigma}{2\varepsilon^2}\frac{\partial H_y}{\partial z}(\tau_{15},x_{i+\frac{1}{2}},y_j,z_{13})-\frac{1}{2\mu\varepsilon}\frac{\partial^2 E_y}{\partial x\partial y}(\tau_{16},x_{11},y_{13},z_k)\Big]\\&+(\Delta t)^2\Big[\frac{1}{24}\frac{\partial^3 E_x}{\partial t^3}(\tau_{11},x_{i+\frac{1}{2}},y_j,z_k)-\frac{1}{8\varepsilon}\frac{\partial^3 H_z}{\partial t^2\partial y}(\tau_{13},x_{i+\frac{1}{2}},y_{12},z_k)\\&+\frac{1}{8\varepsilon}\frac{\partial^3 H_y}{\partial t^2\partial z}(\tau_{14},x_{i+\frac{1}{2}},y_j,z_{12})+\frac{\sigma}{8\varepsilon}\frac{\partial^2 E_x}{\partial t^2}(\tau_{12},x_{i+\frac{1}{2}},y_j,z_k)\Big]\\&-\frac{(\Delta y)^2}{24\varepsilon}\frac{\partial^3 H_z}{\partial y^3}(t^{n+\frac{1}{2}},x_{i+\frac{1}{2}},y_{11},z_k)+\frac{(\Delta z)^2}{24\varepsilon}\frac{\partial^3 H_y}{\partial z^3}(t^{n+\frac{1}{2}},x_{i+\frac{1}{2}},y_j,z_{11})\end{aligned}$$

for some $t^n\le\tau_{11},\cdots,\tau_{16}\le t^{n+1}$, $x_{i-1/2}\le x_{11}\le x_{i+1/2}$, $y_{j-1/2}\le y_{11},y_{12},y_{13}\le y_{j+1/2}$, $z_{k-1/2}\le z_{11},z_{12},z_{13}\le z_{k+1/2}$. Thus,

$$\begin{aligned}&\sum_{i=0}^{I-1}\sum_{j=1}^{J-1}\sum_{k=1}^{K-1}|\xi_{x_{i+\frac{1}{2},j,k}}^{n+\frac{1}{2}}|^2\Delta x\Delta y\Delta z\\ \le&(\Delta t)^2\left[\frac{2\sigma^2}{\varepsilon^4}\|\frac{\partial H_y}{\partial z}\|_\infty^2+\frac{2}{\mu^2\varepsilon^2}\|\frac{\partial^2 E_y}{\partial x\partial y}\|_\infty^2\right]\\&+(\Delta t)^4\left[\|\frac{\partial^3 E_x}{\partial t^3}\|_\infty^2+\frac{1}{\varepsilon^2}\|\frac{\partial^3 H_z}{\partial t^2\partial y}\|_\infty^2+\frac{1}{\varepsilon^2}\|\frac{\partial^3 H_y}{\partial t^2\partial z}\|_\infty^2+\frac{\sigma^2}{\varepsilon^2}\|\frac{\partial^2 E_x}{\partial t^2}\|_\infty^2\right]\\&+\frac{(\Delta y)^4}{\varepsilon^2}\|\frac{\partial^3 H_z}{\partial y^3}\|_\infty^2+\frac{(\Delta z)^4}{\varepsilon^2}\|\frac{\partial^3 H_y}{\partial z^3}\|_\infty^2\\ \le&C_{\mu\varepsilon\sigma^*\sigma}M^2\Big[(\Delta t)^2+(\Delta t)^4+(\Delta y)^4+(\Delta z)^4\Big],\end{aligned}\tag{3.9}$$

where $C_{\mu\varepsilon\sigma^*\sigma}$ is a positive constant depending only on μ, ε, σ and σ^*, and, with the notation $\|f\|_\infty=\|f\|_{L^\infty([0,T];L^2(\Omega))}$ for a scalar function f or $\|\mathbf{f}\|_\infty=\|\mathbf{f}\|_{L^\infty([0,T];[L^2(\Omega)]^3)}$ for a three-dimensional vector function $\mathbf{f}$,

$$\begin{aligned}M\;=\;\max\Big\{&\|\partial_t^2\mathbf{E}\|_\infty,\|\partial_t^3\mathbf{E}\|_\infty,\|\partial_v\partial_u\mathbf{E}\|_\infty,\|\partial_v\mathbf{E}\|_\infty,\|\partial_v^3\mathbf{E}\|_\infty,\|\partial_t\partial_v\mathbf{E}\|_\infty,\\&\|\partial_t^2\mathbf{H}\|_\infty,\|\partial_t^3\mathbf{H}\|_\infty,\|\partial_v\partial_u\mathbf{H}\|_\infty,\|\partial_v\mathbf{H}\|_\infty,\|\partial_v^3\mathbf{H}\|_\infty,\|\partial_t\partial_v\mathbf{H}\|_\infty,u,v=x,y,z\Big\}.\end{aligned}$$

Similar estimates to (3.9) hold for ${\xi_y}^{n+1/2}$, ${\xi_z}^{n+1/2}$, ${\eta_x}^{n+1/2}$, ${\eta_y}^{n+1/2}$ and ${\eta_z}^{n+1/2}$. Now multiplying Eq. (3.6) with $\sqrt{\varepsilon}$ and regrouping the terms, we have

$$\begin{aligned}&\sqrt{\varepsilon}\mathcal{E}_x^{n+1}+\frac{\Delta t}{2\sqrt{\varepsilon}}\delta_z\mathcal{H}_y^{n+1}-\frac{\Delta t}{2\sqrt{\varepsilon}}\Big(\delta_y\mathcal{H}_z^{n+1}+\frac{\Delta t}{2}\delta_y(\frac{1}{\mu}\delta_x\mathcal{E}_y^{n+1})\Big)\\=&\sqrt{\varepsilon}\mathcal{E}_x^{n}-\frac{\Delta t}{2\sqrt{\varepsilon}}\delta_z\mathcal{H}_y^{n}+\frac{\Delta t}{2\sqrt{\varepsilon}}\Big(\delta_y\mathcal{H}_z^{n}+\frac{\Delta t}{2}\delta_y(\frac{1}{\mu}\delta_x\mathcal{E}_y^{n})\Big)\\&-\frac{\sigma\Delta t}{2\sqrt{\varepsilon}}\Big(\mathcal{E}_x^{n+1}+\mathcal{E}_x^{n}+\frac{\Delta t}{2\varepsilon}\delta_z(\mathcal{H}_y^{n+1}+\mathcal{H}_y^{n})\Big)+\Delta t\sqrt{\varepsilon}{\xi_x}^{n+\frac{1}{2}}.\end{aligned}\tag{3.10}$$

Taking the square of both sides of (3.10) and using the inequality

$$(a+\Delta tb)^2 \le (1+\Delta t)(a^2+\Delta tb^2),$$

we obtain that

$$\begin{aligned}
&\beta_1\varepsilon(\mathcal{E}_x^{n+1})^2+\frac{(\Delta t)^2}{4\varepsilon}\beta_1(\delta_z\mathcal{H}_y^{n+1})^2+\frac{(\Delta t)^2}{4\varepsilon}\Big(\delta_y\mathcal{H}_z^{n+1}+\frac{\Delta t}{2}\delta_y(\frac{1}{\mu}\delta_x\mathcal{E}_y^{n+1})\Big)^2\\
&\quad+\Delta t\mathcal{E}_x^{n+1}\cdot\Big(\delta_z\mathcal{H}_y^{n+1}-\delta_y\mathcal{H}_z^{n+1}-\frac{\Delta t}{2}\delta_y(\frac{1}{\mu}\delta_x\mathcal{E}_y^{n+1})\Big)\\
&\quad-\frac{(\Delta t)^2}{2\varepsilon}\delta_z\mathcal{H}_y^{n+1}\cdot\Big(\delta_y\mathcal{H}_z^{n+1}+\frac{\Delta t}{2}\delta_y(\frac{1}{\mu}\delta_x\mathcal{E}_y^{n+1})\Big)\\
\le&(1+\Delta t)\Big\{\beta_2\varepsilon(\mathcal{E}_x^{n})^2+\frac{(\Delta t)^2}{4\varepsilon}\beta_2(\delta_z\mathcal{H}_y^{n})^2+\frac{(\Delta t)^2}{4\varepsilon}\Big(\delta_y\mathcal{H}_z^{n}+\frac{\Delta t}{2}\delta_y(\frac{1}{\mu}\delta_x\mathcal{E}_y^{n})\Big)^2\\
&-\Delta t\mathcal{E}_x^{n}\cdot\Big(\delta_z\mathcal{H}_y^{n}-\delta_y\mathcal{H}_z^{n}-\frac{\Delta t}{2}\delta_y(\frac{1}{\mu}\delta_x\mathcal{E}_y^{n})\Big)\\
&-\frac{(\Delta t)^2}{2\varepsilon}\delta_z\mathcal{H}_y^{n}\cdot\Big(\delta_y\mathcal{H}_z^{n}+\frac{\Delta t}{2}\delta_y(\frac{1}{\mu}\delta_x\mathcal{E}_y^{n})\Big)+5\Delta t\varepsilon(\xi_x^{n+\frac{1}{2}})^2\Big\},
\end{aligned}\tag{3.11}$$

where and in what follows,

$$\begin{aligned}
&\beta_1=1-\frac{5\sigma^2}{4\varepsilon}\Delta t(1+\Delta t),\ \ \beta_2=1+\frac{5\sigma^2}{4\varepsilon}\Delta t,\\
&\gamma_1=1-\frac{5(\sigma^*)^2}{4\mu}\Delta t(1+\Delta t),\ \ \gamma_2=1+\frac{5(\sigma^*)^2}{4\mu}\Delta t.
\end{aligned}$$

Similar procedure can be applied to other error equations to get five inequalities similar to (3.11). Here, for brevity, we only present the inequality for H_y^{n+1}:

$$\begin{aligned}
&\gamma_1\mu(\mathcal{H}_y^{n+1})^2+\frac{(\Delta t)^2}{4\mu}\gamma_1(\delta_z\mathcal{E}_x^{n+1})^2+\frac{(\Delta t)^2}{4\mu}\Big(\delta_x\mathcal{E}_z^{n+1}+\frac{\Delta t}{2}\delta_x(\frac{1}{\varepsilon}\delta_y\mathcal{H}_x^{n+1})\Big)^2\\
&\quad+\Delta t\mathcal{H}_y^{n+1}\cdot\Big(\delta_z\mathcal{E}_x^{n+1}-\delta_x\mathcal{E}_z^{n+1}-\frac{\Delta t}{2}\delta_x(\frac{1}{\varepsilon}\delta_y\mathcal{H}_x^{n+1})\Big)\\
&\quad-\frac{(\Delta t)^2}{2\mu}\delta_z\mathcal{E}_x^{n+1}\cdot\Big(\delta_x\mathcal{E}_z^{n+1}+\frac{\Delta t}{2}\delta_x(\frac{1}{\varepsilon}\delta_y\mathcal{H}_x^{n+1})\Big)\\
\le&(1+\Delta t)\Big\{\mu\gamma_2(\mathcal{H}_y^{n})^2+\frac{(\Delta t)^2}{4\mu}\gamma_2(\delta_z\mathcal{E}_x^{n})^2+\frac{(\Delta t)^2}{4\mu}\Big(\delta_x\mathcal{E}_z^{n}+\frac{\Delta t}{2}\delta_x(\frac{1}{\varepsilon}\delta_y\mathcal{H}_x^{n})\Big)^2\\
&-\Delta t\mathcal{H}_y^{n}\cdot\Big(\delta_z\mathcal{E}_x^{n}-\delta_x\mathcal{E}_z^{n}-\frac{\Delta t}{2}\delta_x(\frac{1}{\varepsilon}\delta_y\mathcal{H}_x^{n})\Big)\\
&-\frac{(\Delta t)^2}{2\mu}\delta_z\mathcal{E}_x^{n}\cdot\Big(\delta_x\mathcal{E}_z^{n}+\frac{\Delta t}{2}\delta_x(\frac{1}{\varepsilon}\delta_y\mathcal{H}_x^{n})\Big)+5\Delta t\mu(\eta_y^{n+\frac{1}{2}})^2\Big\},
\end{aligned}\tag{3.12}$$

and

$$
\begin{aligned}
&\mu\gamma_1(\mathcal{H}_z^{n+1})^2+\frac{(\Delta t)^2}{4\mu}\gamma_1(\delta_x\mathcal{E}_y^{n+1})^2+\frac{(\Delta t)^2}{4\mu}\Big(\delta_y\mathcal{E}_x^{n+1}+\frac{\Delta t}{2}\delta_y(\frac{1}{\varepsilon}\delta_z\mathcal{H}_y^{n+1})\Big)^2\\
&\quad+\Delta t\mathcal{H}_z^{n+1}\cdot\Big(\delta_x\mathcal{E}_y^{n+1}-\delta_y\mathcal{E}_x^{n+1}-\frac{\Delta t}{2}\delta_y(\frac{1}{\varepsilon}\delta_z\mathcal{H}_y^{n+1})\Big)\\
&\quad-\frac{(\Delta t)^2}{2\mu}\delta_x\mathcal{E}_y^{n+1}\cdot\Big(\delta_y\mathcal{E}_x^{n+1}+\frac{\Delta t}{2}\delta_y(\frac{1}{\varepsilon}\delta_z\mathcal{H}_y^{n+1})\Big)\\
\le&(1+\Delta t)\Big\{\mu\gamma_2(\mathcal{H}_z^{n})^2+\frac{(\Delta t)^2}{4\mu}\gamma_2(\delta_x\mathcal{E}_y^{n})^2+\frac{(\Delta t)^2}{4\mu}\Big(\delta_y\mathcal{E}_x^{n}+\frac{\Delta t}{2}\delta_y(\frac{1}{\varepsilon}\delta_z\mathcal{H}_y^{n})\Big)^2\\
&-\Delta t\mathcal{H}_z^{n}\cdot\Big(\delta_x\mathcal{E}_y^{n}-\delta_y\mathcal{E}_x^{n}-\frac{\Delta t}{2}\delta_y(\frac{1}{\varepsilon}\delta_z\mathcal{H}_y^{n})\Big)\\
&-\frac{(\Delta t)^2}{2\varepsilon}\delta_x\mathcal{E}_y^{n}\cdot\Big(\delta_y\mathcal{E}_x^{n}+\frac{\Delta t}{2}\delta_y(\frac{1}{\varepsilon}\delta_z\mathcal{H}_y^{n})\Big)+5\Delta t\mu(\eta_z^{n+\frac{1}{2}})^2\Big\}. \qquad (3.13)
\end{aligned}
$$

The sums over i,j,k in their corresponding valid ranges of the mixed product terms on the left-hand (or right-hand) sides of the six inequalities thus obtained (including (3.11)-(3.13)) can be shown to be canceled out with each other by using summation by parts and the boundary conditions (2.20)-(2.22). For example, consider the sums of the mixed product terms on the left-hand sides of (3.11)-(3.12). By summation by parts it follows that

$$
\begin{aligned}
&\sum_{i=0}^{I-1}\sum_{j=1}^{J-1}\sum_{k=0}^{K-1}\Delta t\,\mathcal{H}^{n+1}_{y_{i+\frac{1}{2},j,k+\frac{1}{2}}}\cdot\delta_z\mathcal{E}^{n+1}_{x_{i+\frac{1}{2},j,k+\frac{1}{2}}}\\
=&\sum_{i=0}^{I-1}\sum_{j=1}^{J-1}\frac{\Delta t}{\Delta z}\Big[\mathcal{H}^{n+1}_{y_{i+\frac{1}{2},j,K-\frac{1}{2}}}\mathcal{E}^{n+1}_{x_{i+\frac{1}{2},j,K}}-\mathcal{H}^{n+1}_{y_{i+\frac{1}{2},j,\frac{1}{2}}}\mathcal{E}^{n+1}_{x_{i+\frac{1}{2},j,0}}\\
&-\sum_{k=1}^{K-1}\mathcal{E}^{n+1}_{x_{i+\frac{1}{2},j,k}}(\mathcal{H}^{n+1}_{y_{i+\frac{1}{2},j,k+\frac{1}{2}}}-\mathcal{H}^{n+1}_{y_{i+\frac{1}{2},j,k-\frac{1}{2}}})\Big]\\
=&\sum_{i=0}^{I-1}\sum_{j=1}^{J-1}\sum_{k=1}^{K-1}\Delta t\,\mathcal{E}^{n+1}_{x_{i+\frac{1}{2},j,k}}\delta_z\mathcal{H}^{n+1}_{y_{i+\frac{1}{2},j,k}}, \qquad (3.14)
\end{aligned}
$$

where we have used the boundary conditions (2.20)-(2.22) that

$$
\begin{aligned}
&\mathcal{E}^{n+\frac{1}{2}}_{x_{i+\frac{1}{2},j,0}}=\mathcal{E}^{n+\frac{1}{2}}_{x_{i+\frac{1}{2},j,K}}=\mathcal{E}^{n+\frac{1}{2}}_{x_{i+\frac{1}{2},0,k}}=\mathcal{E}^{n+\frac{1}{2}}_{x_{i+\frac{1}{2},J,k}}=0,\\
&\mathcal{E}^{n+\frac{1}{2}}_{y_{0,j+\frac{1}{2},k}}=\mathcal{E}^{n+\frac{1}{2}}_{y_{I,j+\frac{1}{2},k}}=\mathcal{E}^{n+\frac{1}{2}}_{y_{i,j+\frac{1}{2},0}}=\mathcal{E}^{n+\frac{1}{2}}_{y_{i,j+\frac{1}{2},K}}=0, \qquad (3.15)\\
&\mathcal{E}^{n+\frac{1}{2}}_{z_{0,j,k+\frac{1}{2}}}=\mathcal{E}^{n+\frac{1}{2}}_{z_{I,j,k+\frac{1}{2}}}=\mathcal{E}^{n+\frac{1}{2}}_{z_{i,0,k+\frac{1}{2}}}=\mathcal{E}^{n+\frac{1}{2}}_{z_{i,J,k+\frac{1}{2}}}=0
\end{aligned}
$$

for all valid values of i,j,k. This means that the sum over i,j,k in their valid ranges of the first mixed product term on the left-hand side of (3.12) plus that of the first mixed product term on the left-hand side of (3.11) is equal to zero. Similar argument can be used to show that the sum over i,j,k in their valid ranges of the second mixed product term on the left-hand side of (3.13) plus the sum over i,j,k in their valid ranges of the second mixed product term on the left-hand side of (3.11) equals zero.

Now consider the fourth mixed product term on the left-hand side of (3.13). By summation by parts and the boundary conditions (3.15) it is seen that

$$
\begin{aligned}
&-\sum_{i=0}^{I-1}\sum_{j=0}^{J-1}\sum_{k=1}^{K-1}\frac{(\Delta t)^2}{2\mu}\delta_x\mathcal{E}^{n+1}_{y_{i+\frac12,j+\frac12,k}}\delta_y\mathcal{E}^{n+1}_{x_{i+\frac12,j+\frac12,k}}\\
=&-\sum_{i=0}^{I-1}\sum_{k=1}^{K-1}\frac{(\Delta t)^2}{2\Delta y}\Big[\frac{1}{\mu}\delta_x\mathcal{E}^{n+1}_{y_{i+\frac12,J-\frac12,k}}\mathcal{E}^{n+1}_{x_{i+\frac12,J,k}}-\frac{1}{\mu}\delta_x\mathcal{E}^{n+1}_{y_{i+\frac12,\frac12,k}}\mathcal{E}^{n+1}_{x_{i+\frac12,0,k}}\\
&-\sum_{j=1}^{J-1}\mathcal{E}^{n+1}_{x_{i+\frac12,j,k}}\big(\frac{1}{\mu}\delta_x\mathcal{E}^{n+1}_{y_{i+\frac12,j+\frac12,k}}-\frac{1}{\mu}\delta_x\mathcal{E}^{n+1}_{y_{i+\frac12,j-\frac12,k}}\big)\Big]\\
=&\sum_{i=0}^{I-1}\sum_{j=1}^{J-1}\sum_{k=1}^{K-1}\frac{(\Delta t)^2}{2\mu}\mathcal{E}^{n+1}_{x_{i+\frac12,j,k}}\delta_y\big(\frac{1}{\mu}\delta_x\mathcal{E}^{n+1}_{y_{i+\frac12,j,k}}\big),
\end{aligned}\tag{3.16}
$$

which plus the sum over i,j,k in their valid ranges of the third mixed product term on the left-hand side of (3.11) is zero. Next, the sum of the third mixed term on the left-hand side of (3.13) is

$$
\begin{aligned}
&-\sum_{i=0}^{I-1}\sum_{j=0}^{J-1}\sum_{k=1}^{K-1}\Delta t\mathcal{H}^{n+1}_{z_{i+\frac12,j+\frac12,k}}\cdot\frac{\Delta t}{2}\delta_y\Big(\frac{1}{\varepsilon}\delta_z\mathcal{H}^{n+1}_{y_{i+\frac12,j+\frac12,k}}\Big)\\
=&-\sum_{i=0}^{I-1}\sum_{k=1}^{K-1}\frac{(\Delta t)^2}{2\Delta y}\Big[\mathcal{H}^{n+1}_{z_{i+\frac12,J-\frac12,k}}\cdot\frac{1}{\varepsilon}\delta_z\mathcal{H}^{n+1}_{y_{i+\frac12,J,k}}-\mathcal{H}^{n+1}_{z_{i+\frac12,\frac12,k}}\cdot\frac{1}{\varepsilon}\delta_z\mathcal{H}^{n+1}_{y_{i+\frac12,0,k}}\\
&-\sum_{j=1}^{J-1}\frac{1}{\varepsilon}\delta_z\mathcal{H}^{n+1}_{y_{i+\frac12,j,k}}\cdot\big(\mathcal{H}^{n+1}_{z_{i+\frac12,j+\frac12,k}}-\mathcal{H}^{n+1}_{z_{i+\frac12,j-\frac12,k}}\big)\Big]\\
=&\sum_{i=0}^{I-1}\sum_{j=1}^{J-1}\sum_{k=1}^{K-1}\frac{(\Delta t)^2}{2\varepsilon}\delta_z\mathcal{H}^{n+1}_{y_{i+\frac12,j,k}}\cdot\delta_y\mathcal{H}^{n+1}_{z_{i+\frac12,j,k}},
\end{aligned}\tag{3.17}
$$

which plus the sum over i,j,k in their valid ranges of the fourth mixed product term on the left-hand side of (3.11) equals zero, where we have used the following boundary conditions which follows from the boundary condition (2.6):

$$
\begin{aligned}
&\mathcal{H}^n_{x_{0,j+\frac12,k+\frac12}}=\mathcal{H}^n_{x_{I,j+\frac12,k+\frac12}}=0,\quad\forall j,k,n;\\
&\mathcal{H}^n_{y_{i+\frac12,0,k+\frac12}}=\mathcal{H}^n_{y_{i+\frac12,J,k+\frac12}}=0,\quad\forall i,k,n;\\
&\mathcal{H}^n_{z_{i+\frac12,j+\frac12,0}}=\mathcal{H}^n_{z_{i+\frac12,j+\frac12,K}}=0,\quad\forall i,j,n.
\end{aligned}
$$

Using the above boundary conditions and summation by parts again we have for the sum of the last mixed product term on the left-hand side of (3.13) that

$$
\begin{aligned}
&-\sum_{i=0}^{I-1}\sum_{j=0}^{J-1}\sum_{k=1}^{K-1}\frac{(\Delta t)^2}{2\mu}\delta_x\mathcal{E}^{n+1}_{y_{i+\frac12,j+\frac12,k}}\cdot\frac{\Delta t}{2}\delta_y\Big(\frac{1}{\varepsilon}\delta_z\mathcal{H}^{n+1}_{y_{i+\frac12,j+\frac12,k}}\Big)\\
=&-\sum_{i=0}^{I-1}\sum_{k=1}^{K-1}\frac{(\Delta t)^3}{4\Delta y}\Big[\frac{1}{\mu}\delta_x\mathcal{E}^{n+1}_{y_{i+\frac12,J-\frac12,k}}\cdot\frac{1}{\varepsilon}\delta_z\mathcal{H}^{n+1}_{y_{i+\frac12,J,k}}-\frac{1}{\mu}\delta_x\mathcal{E}^{n+1}_{y_{i+\frac12,\frac12,k}}\cdot\frac{1}{\varepsilon}\delta_z\mathcal{H}^{n+1}_{y_{i+\frac12,0,k}}\\
&-\sum_{j=1}^{J-1}\frac{1}{\varepsilon}\delta_z\mathcal{H}^{n+1}_{y_{i+\frac12,j,k}}\cdot(\frac{1}{\mu}\delta_x\mathcal{E}^{n+1}_{y_{i+\frac12,j+\frac12,k}}-\frac{1}{\mu}\delta_x\mathcal{E}^{n+1}_{y_{i+\frac12,j-\frac12,k}})\Big]\\
=&\sum_{i=0}^{I-1}\sum_{j=1}^{J-1}\sum_{k=1}^{K-1}\frac{(\Delta t)^3}{4\varepsilon}\,\delta_z\mathcal{H}^{n+1}_{y_{i+\frac12,j,k}}\cdot\delta_y\Big(\frac{1}{\mu}\delta_x\mathcal{E}^{n+1}_{y_{i+\frac12,j,k}}\Big),
\end{aligned}
\tag{3.18}
$$

which cancels out the sum over i,j,k in their valid ranges of the last mixed product term on the left-hand side of (3.11). Thus all mixed product terms on the left-hand side of (3.11) are cancelled out by some terms on the left-hand side of (3.12)-(3.13) when the sums are taken over i,j,k in their valid ranges. By a similar argument it can be shown that the sums over i,j,k in their valid ranges of the other mixed product terms on both sides of the six inequalities can also be cancelled out with each other. Thus, summing each of the six inequalities (including (3.11)-(3.13)) up over i,j,k in their valid ranges and then adding the updated six inequalities together, we arrive at

$$
\begin{aligned}
&\sum_{i,j,k}\Big[\varepsilon\beta_1(\mathcal{E}^{n+1}_x)^2+\frac{(\Delta t)^2}{4\varepsilon}\beta_1(\delta_z\mathcal{H}^{n+1}_y)^2+\frac{(\Delta t)^2}{4\varepsilon}\Big(\delta_y\mathcal{H}^{n+1}_z+\frac{\Delta t}{2}\delta_y(\frac{1}{\mu}\delta_x\mathcal{E}^{n+1}_y)\Big)^2\Big]\\
&+\sum_{i,j,k}\Big[\varepsilon\beta_1(\mathcal{E}^{n+1}_y)^2+\frac{(\Delta t)^2}{4\varepsilon}\beta_1(\delta_x\mathcal{H}^{n+1}_z)^2+\frac{(\Delta t)^2}{4\varepsilon}\Big(\delta_z\mathcal{H}^{n+1}_x+\frac{\Delta t}{2}\delta_z(\frac{1}{\mu}\delta_y\mathcal{E}^{n+1}_z)\Big)^2\Big]\\
&+\sum_{i,j,k}\Big[\varepsilon\beta_1(\mathcal{E}^{n+1}_z)^2+\frac{(\Delta t)^2}{4\varepsilon}\beta_1(\delta_y\mathcal{H}^{n+1}_x)^2+\frac{(\Delta t)^2}{4\varepsilon}\Big(\delta_x\mathcal{H}^{n+1}_y+\frac{\Delta t}{2}\delta_x(\frac{1}{\mu}\delta_z\mathcal{E}^{n+1}_x)\Big)^2\Big]\\
&+\sum_{i,j,k}\Big[\mu\gamma_1(\mathcal{H}^{n+1}_x)^2+\frac{(\Delta t)^2}{4\mu}\gamma_1(\delta_y\mathcal{E}^{n+1}_z)^2+\frac{(\Delta t)^2}{4\mu}\Big(\delta_z\mathcal{E}^{n+1}_y+\frac{\Delta t}{2}\delta_z(\frac{1}{\varepsilon}\delta_x\mathcal{H}^{n+1}_z)\Big)^2\Big]\\
&+\sum_{i,j,k}\Big[\mu\gamma_1(\mathcal{H}^{n+1}_y)^2+\frac{(\Delta t)^2}{4\mu}\gamma_1(\delta_z\mathcal{E}^{n+1}_x)^2+\frac{(\Delta t)^2}{4\mu}\Big(\delta_x\mathcal{E}^{n+1}_z+\frac{\Delta t}{2}\delta_x(\frac{1}{\varepsilon}\delta_y\mathcal{H}^{n+1}_x)\Big)^2\Big]\\
&+\sum_{i,j,k}\Big[\mu\gamma_1(\mathcal{H}^{n+1}_z)^2+\frac{(\Delta t)^2}{4\mu}\gamma_1(\delta_x\mathcal{E}^{n+1}_y)^2+\frac{(\Delta t)^2}{4\mu}\Big(\delta_y\mathcal{E}^{n+1}_x+\frac{\Delta t}{2}\delta_y(\frac{1}{\varepsilon}\delta_z\mathcal{H}^{n+1}_y)\Big)^2\Big]
\end{aligned}
$$

$$
\begin{aligned}
&\le (1+\Delta t)\Big\{\sum_{i,j,k}\Big[\varepsilon\beta_2(\mathcal{E}_x^n)^2+\frac{(\Delta t)^2}{4\varepsilon}\beta_2(\delta_z\mathcal{H}_y^n)^2\\
&\quad+\frac{(\Delta t)^2}{4\varepsilon}\Big(\delta_y\mathcal{H}_z^n+\frac{\Delta t}{2}\delta_y(\frac{1}{\mu}\delta_x\mathcal{E}_y^n)\Big)^2+5\Delta t\varepsilon(\xi_x^{n+\frac{1}{2}})^2\Big]\\
&\quad+\sum_{i,j,k}\Big[\varepsilon\beta_2(\mathcal{E}_y^n)^2+\frac{(\Delta t)^2}{4\varepsilon}\beta_2(\delta_x\mathcal{H}_z^n)^2+\frac{(\Delta t)^2}{4\varepsilon}\Big(\delta_z\mathcal{H}_x^n+\frac{\Delta t}{2}\delta_z(\frac{1}{\mu}\delta_y\mathcal{E}_z^n)\Big)^2+5\Delta t\varepsilon(\xi_y^{n+\frac{1}{2}})^2\Big]\\
&\quad+\sum_{i,j,k}\Big[\varepsilon\beta_2(\mathcal{E}_z^n)^2+\frac{(\Delta t)^2}{4\varepsilon}\beta_2(\delta_y\mathcal{H}_x^n)^2+\frac{(\Delta t)^2}{4\varepsilon}\Big(\delta_x\mathcal{H}_y^n+\frac{\Delta t}{2}\delta_x(\frac{1}{\mu}\delta_z\mathcal{E}_x^n)\Big)^2+5\Delta t\varepsilon(\xi_z^{n+\frac{1}{2}})^2\Big]\\
&\quad+\sum_{i,j,k}\Big[\mu\gamma_2(\mathcal{H}_x^n)^2+\frac{(\Delta t)^2}{4\mu}\gamma_2(\delta_y\mathcal{E}_z^n)^2+\frac{(\Delta t)^2}{4\mu}\Big(\delta_z\mathcal{E}_y^n+\frac{\Delta t}{2}\delta_z(\frac{1}{\varepsilon}\delta_x\mathcal{H}_z^n)\Big)^2+5\Delta t\mu(\eta_x^{n+\frac{1}{2}})^2\Big]\\
&\quad+\sum_{i,j,k}\Big[\mu\gamma_2(\mathcal{H}_y^n)^2+\frac{(\Delta t)^2}{4\mu}\gamma_2(\delta_z\mathcal{E}_x^n)^2+\frac{(\Delta t)^2}{4\mu}\Big(\delta_x\mathcal{E}_z^n+\frac{\Delta t}{2}\delta_x(\frac{1}{\varepsilon}\delta_y\mathcal{H}_x^n)\Big)^2+5\Delta t\mu(\eta_y^{n+\frac{1}{2}})^2\Big]\\
&\quad+\sum_{i,j,k}\Big[\mu\gamma_2(\mathcal{H}_z^n)^2+\frac{(\Delta t)^2}{4\mu}\gamma_2(\delta_x\mathcal{E}_y^n)^2+\frac{(\Delta t)^2}{4\mu}\Big(\delta_y\mathcal{E}_x^n+\frac{\Delta t}{2}\delta_y(\frac{1}{\varepsilon}\delta_z\mathcal{H}_y^n)\Big)^2\\
&\qquad+5\Delta t\mu(\eta_z^{n+\frac{1}{2}})^2\Big]\Big\},
\end{aligned}
\tag{3.19}
$$

where the summation is for $0\le i\le I-1$, $0\le j\le J-1$ and $0\le k\le K-1$. Let

$$
\alpha=\max\Big\{\frac{5\sigma^2}{4\varepsilon},\frac{5(\sigma^*)^2}{4\mu},\frac{5\sigma^2}{4\varepsilon}(1+\Delta t),\frac{5(\sigma^*)^2}{4\mu}(1+\Delta t)\Big\}. \tag{3.20}
$$

Then β_1 and γ_1 are greater than $1-\alpha\Delta t$ and β_2 and γ_2 are less than $1+\alpha\Delta t$. So, multiplying the above inequality with $(1-\alpha\Delta t)^{-1}\Delta x\Delta y\Delta z$ and using the estimates of the local truncation errors it follows on noting the definitions of δ_1^h, δ_2^h and the energy norm that the above inequality can be written as

$$
\begin{aligned}
&\|\varepsilon^{\frac{1}{2}}\mathcal{E}^{n+1}\|_E^2+\|\mu^{\frac{1}{2}}\mathcal{H}^{n+1}\|_H^2+\frac{(\Delta t)^2}{4}\Big(\|\varepsilon^{-\frac{1}{2}}\delta_2^h\mathcal{H}^{n+1}\|_E^2+\|\mu^{-\frac{1}{2}}\delta_1^h\mathcal{E}^{n+1}\|_H^2\Big)\\
&\quad+\frac{(\Delta t)^2}{4}\Big(\|\varepsilon^{-\frac{1}{2}}(\delta_1^h\mathcal{H}^{n+1}+\frac{\Delta t}{2}\delta_1^h(\frac{1}{\mu}\delta_1^h\mathcal{E}^{n+1}))\|_E^2+\|\mu^{-\frac{1}{2}}(\delta_2^h\mathcal{E}^{n+1}+\frac{\Delta t}{2}\delta_2^h(\frac{1}{\varepsilon}\delta_2^h\mathcal{H}^{n+1}))\|_H^2\Big)\\
&\le(1+\Delta t)(1+\alpha^*\Delta t)\Big\{\|\varepsilon^{\frac{1}{2}}\mathcal{E}^n\|_E^2+\|\mu^{\frac{1}{2}}\mathcal{H}^n\|_H^2+\frac{(\Delta t)^2}{4}\Big(\|\varepsilon^{-\frac{1}{2}}\delta_2^h\mathcal{H}^n\|_E^2+\|\mu^{-\frac{1}{2}}\delta_1^h\mathcal{E}^n\|_H^2\Big)\\
&\quad+\frac{(\Delta t)^2}{4}\Big(\|\varepsilon^{-\frac{1}{2}}(\delta_1^h\mathcal{H}^n+\frac{\Delta t}{2}\delta_1^h(\frac{1}{\mu}\delta_1^h\mathcal{E}^n))\|_E^2+\|\mu^{-\frac{1}{2}}(\delta_2^h\mathcal{E}^n+\frac{\Delta t}{2}\delta_2^h(\frac{1}{\varepsilon}\delta_2^h\mathcal{H}^n))\|_H^2\Big)\\
&\quad+C_1\Delta t[(\Delta t)^2+(\Delta x)^4+(\Delta y)^4+(\Delta z)^4]\Big\},
\end{aligned}
\tag{3.21}
$$

where $(1+\alpha\Delta t)/(1-\alpha\Delta t)=1+\alpha^*\Delta t$ with

$$
\alpha^*=2\alpha/(1-\alpha\Delta t),\quad C_1=30\max(\varepsilon,\mu)C_{\mu\varepsilon\sigma^*\sigma}M^2.
$$

A successive application of the above inequality gives

$$
\begin{aligned}
&\text{LHS of (3.21)}\\
\le&(1+\Delta t)^{n+1}(1+\alpha^*\Delta t)^{n+1}\Big\{\|\varepsilon^{\frac{1}{2}}\mathcal{E}^0\|_E^2+\|\mu^{\frac{1}{2}}\mathcal{H}^0\|_H^2+\frac{(\Delta t)^2}{4}\Big(\|\varepsilon^{-\frac{1}{2}}\delta_2^h\mathcal{H}^0\|_E^2\\
&+\|\mu^{-\frac{1}{2}}\delta_1^h{\mathcal{E}_x}^0\|_H^2+\|\varepsilon^{-\frac{1}{2}}(\delta_1^h\mathcal{H}^0+\frac{\Delta t}{2}\delta_1^h(\frac{1}{\mu}\delta_1^h{\mathcal{E}_x}^0))\|_E^2+\|\mu^{-\frac{1}{2}}(\delta_2^h\mathcal{E}^0+\frac{\Delta t}{2}\delta_2^h(\frac{1}{\varepsilon}\delta_2^h\mathcal{H}^0))\|_H^2\Big)\\
&+C_1(n+1)\Delta t[(\Delta t)^2+(\Delta x)^4+(\Delta y)^4+(\Delta z)^4]\Big\}\\
\le&C[(\Delta t)^2+(\Delta x)^4+(\Delta y)^4+(\Delta z)^4],
\end{aligned}
\tag{3.22}
$$

where

$$C=2C_1T(1+T)(1+\alpha^*T)e^{T(\alpha^*+1)}$$

is bounded above with a bound independent of Δt, which implies (3.1).

To prove (3.2), subtracting each equation in (3.6)-(3.8) and the relevant equations for H_x, H_y, H_z with n replaced by $n-1$ from itself, respectively, will give six new error equations. Then (3.2) can be derived by repeating the above argument starting from the new error equations. Theorem 3.1 is thus proved. □

A similar argument as above can be used to show the following theorem on the stability of the splitting scheme S-FDTD.

Theorem 3.2. *Let $n\ge 0$ and let*

$$\mathbf{E}^n=(E^n_{x_{i+\frac{1}{2},j,k}},E^n_{y_{i,j+\frac{1}{2},k}},E^n_{z_{i,j,k+\frac{1}{2}}}),\qquad \mathbf{H}^n=(H^n_{x_{i,j+\frac{1}{2},k+\frac{1}{2}}},H^n_{y_{i+\frac{1}{2},j,k+\frac{1}{2}}},H^n_{z_{i+\frac{1}{2},j+\frac{1}{2},k}})$$

be the solution of the splitting scheme S-FDTD. Then

$$
\begin{aligned}
&\|\varepsilon^{\frac{1}{2}}\mathbf{E}^{n+1}\|_E^2+\|\mu^{\frac{1}{2}}\mathbf{H}^{n+1}\|_H^2\\
\le&\|\varepsilon^{\frac{1}{2}}\mathbf{E}^0\|_E^2+\|\mu^{\frac{1}{2}}\mathbf{H}^0\|_H^2+\frac{(\Delta t)^2}{4}\Big(\|\varepsilon^{-\frac{1}{2}}\delta_2^h\mathbf{H}^0\|_E^2+\|\mu^{-\frac{1}{2}}\delta_1^h\mathbf{E}^0\|_H^2\\
&+\|\varepsilon^{-\frac{1}{2}}\Big[\delta_1^h\mathbf{H}^0+\frac{\Delta t}{2\mu}(\delta_1^h)^2\mathbf{E}^0\Big]\|_E^2+\|\mu^{-\frac{1}{2}}\Big[\delta_2^h\mathbf{E}^0+\frac{\Delta t}{2\varepsilon}(\delta_2^h)^2\mathbf{H}^0\Big]\|_H^2\Big),\\
&\|\varepsilon^{\frac{1}{2}}\delta_t\mathbf{E}^{n+\frac{1}{2}}\|_E^2+\|\mu^{\frac{1}{2}}\delta_t\mathbf{H}^{n+\frac{1}{2}}\|_H^2\\
\le&\|\varepsilon^{\frac{1}{2}}\delta_t\mathbf{E}^{\frac{1}{2}}\|_E^2+\|\mu^{\frac{1}{2}}\delta_t\mathbf{H}^{\frac{1}{2}}\|_H^2+\frac{(\Delta t)^2}{4}\Big(\|\varepsilon^{-\frac{1}{2}}\delta_2^h\delta_t\mathbf{H}^{\frac{1}{2}}\|_E^2+\|\mu^{-\frac{1}{2}}\delta_1^h\delta_t\mathbf{E}^{\frac{1}{2}}\|_H^2\\
&+\|\varepsilon^{-\frac{1}{2}}\delta_t\Big[\delta_1^h\mathbf{H}^{\frac{1}{2}}+\frac{\Delta t}{2\mu}(\delta_1^h)^2\mathbf{E}^{\frac{1}{2}}\Big]\|_E^2+\|\mu^{-\frac{1}{2}}\delta_t\Big[\delta_2^h\mathbf{E}^{\frac{1}{2}}+\frac{\Delta t}{2\varepsilon}(\delta_2^h)^2\mathbf{H}^{\frac{1}{2}}\Big]\|_H^2\Big).
\end{aligned}
$$

This means that the splitting scheme S-FDTD is unconditionally stable.

Remark 3.1. Theorems 3.1 and 3.2 remain true for the case of variable coefficients ε,μ,σ and σ^* provided ε and μ are strictly positive continuous functions on $\bar{\Omega}$ and σ and σ^* are nonnegative continuous functions on $\bar{\Omega}$ (and the required smoothness on $\mathbf{E}$ and $\mathbf{H}$ is present). In fact, in this case, the same argument as in the proof of Theorem 3.1 still works.

Remark 3.2. The error estimates in Theorem 3.1 depend on strong spatial smoothness assumptions on the solutions of the Maxwell equations. The spatial smoothness restrictions on $\mathbf{E}$ and $\mathbf{H}$ might be reduced to Sobolev space bounds if the Bramble-Hilbert lemma, rather than the Taylor series remainder, is used to bound the error terms.

4 Dispersion and dissipation properties of the two schemes

In this section, we study the dispersion and dissipation properties of the two splitting schemes using a Fourier analysis. To this end, let us assume that $\sigma=\sigma^*=0$ and ε and μ are constant, that is, the isotropic medium is lossless and homogeneous. Let

$$\mathbf{E}^n_{\alpha,\beta,\gamma}=\hat{\mathbf{E}}\xi^n e^{-i(\alpha k_x\Delta x+\beta k_y\Delta y+\gamma k_z\Delta z)},\qquad \mathbf{H}^n_{\alpha,\beta,\gamma}=\hat{\mathbf{H}}\xi^n e^{-i(\alpha k_x\Delta x+\beta k_y\Delta y+\gamma k_z\Delta z)},$$

where the complex-valued vectors $\hat{\mathbf{E}}$ is the eigenvector of the equivalent scheme (2.31)-(2.33) of the scheme IS-FDTD, $\hat{\mathbf{H}}$ is the corresponding eigenvalue for $\mathbf{H}$, ξ is the complex time eigenvalue (or stability factor) we wish to find out and whose magnitude will determine the stability and dissipation properties of the scheme IS-FDTD. Substituting them into (2.31)-(2.33) yields a homogeneous algebraic system with a non-zero solution $\hat{\mathbf{E}}$. Similar system can be obtained for $\hat{\mathbf{H}}$. It is known that the determinant of the coefficient matrix should be zero. A straightforward but tedious calculation leads to the characteristic polynomial equation for ξ:

$$(\xi-1)^2\,(\beta_2\,\xi^2+2\,\beta_1\,\xi+\beta_0)^2=0, \tag{4.1}$$

where

$$\begin{aligned}
&\beta_2=\beta_0=1+\gamma_1+\gamma_2+(c\Delta t)^6(a_x)^2(b_y)^2(c_z)^2,\\
&\beta_1=-1+\gamma_1+\gamma_2-(c\Delta t)^6(a_x)^2(b_y)^2(c_z)^2,\\
&a_x=\frac{\sin(\frac{1}{2}k_x\Delta x)}{\Delta x},\quad b_y=\frac{\sin(\frac{1}{2}k_y\Delta y)}{\Delta y},\quad c_z=\frac{\sin(\frac{1}{2}k_z\Delta z)}{\Delta z}.
\end{aligned}$$

In the definitions of β_1 and β_2,

$$\gamma_1=(c\Delta t)^2[(a_x)^2+(b_y)^2+(c_z)^2],\quad \gamma_2=(c\Delta t)^4[(a_xb_y)^2+(b_yc_z)^2+(c_za_x)^2]. \tag{4.2}$$

Eq. (4.1) has exactly six roots:

$$\begin{aligned}
&\xi_1=\xi_2=1,\ \xi_3=\xi_4=(\beta_2)^{-1}[-\beta_1+i\sqrt{(\beta_2)^2-(\beta_1)^2}],\\
&\xi_5=\xi_6=(\beta_2)^{-1}[-\beta_1-i\sqrt{(\beta_2)^2-(\beta_1)^2}].
\end{aligned}$$

It is clear that the moduli of the six roots are equal to unity. This means that the scheme IS-FDTD is unconditionally stable and non-dissipative.

Similarly, we can derive the characteristic polynomial equation for the splitting scheme S-FDTD:

$$(\alpha_3\,\xi^3+\alpha_2\,\xi^2+\alpha_1\,\xi+\alpha_0)^2=0, \tag{4.3}$$

where

$$\begin{aligned}
\alpha_3 &= 1+\gamma_1+\gamma_2+(c\Delta t)^6(a_x)^2(b_y)^2(c_z)^2,\\
\alpha_2 &= -3+\gamma_1+3\gamma_2+3(c\Delta t)^6(a_x)^2(b_y)^2(c_z)^2,\\
\alpha_1 &= 3-\gamma_1+3\gamma_2+3(c\Delta t)^6(a_x)^2(b_y)^2(c_z)^2,\\
\alpha_0 &= -1-\gamma_1+\gamma_2+(c\Delta t)^6(a_x)^2(b_y)^2(c_z)^2,
\end{aligned}$$

where γ_1 and γ_2 are given by (4.2). The three repeated roots (one real and two complex) can still be expressed explicitly but are very complicated. So we omit them here but plot $|\xi|$ numerically in Figs. 1 and 2 below. To this end, let

$$\begin{aligned}
&k_x=k\sin(\phi)\cos(\theta), \quad k_y=k\sin(\phi)\sin(\theta), \quad k_z=k\cos(\phi),\\
&k^2=(k_x)^2+(k_y)^2+(k_z)^2, \quad N_\lambda=\frac{\lambda}{h}, \quad \omega=ck, \qquad S=c\Delta t/h.
\end{aligned}$$

Then k is the wave number, θ and ϕ are the wave propagation angles, λ is the wavelength, N_λ is the number of points per wavelength (NPPW) (we assume here that $\Delta x=\Delta y=\Delta z=h$), and $\sqrt{3}S$ is the Courant (or CFL) number.

Fig. 1 shows the modulus of the three roots ξ of the polynomial equation (4.3) (or the stability factor) for the splitting scheme S-FDTD as a function of the propagation angle θ at a CFL number $\sqrt{3}S=1.5\sqrt{3}$ in the case with $N_\lambda=30$ (number of points per wavelength) and $\phi=45^\circ$ (left picture), and as a function of the propagation angle ϕ in the case with $\theta=35^\circ$, the number of points per wavelength $N_\lambda=40$ and $S=1.4$ (the CFL number is $\sqrt{3}S$) (right picture). Fig. 2 presents the modulus of the three roots ξ of (4.3) for S-FDTD as a function of S (the CFL number is $\sqrt{3}S$) in the case with the number of points per wavelength $N_\lambda=60$, $\theta=65^\circ$ and $\phi=35^\circ$ (left picture), and as a function of N_λ (the number of points per wavelength) in the case with $\theta=65^\circ$, $\phi=35^\circ$ and the CFL number $\sqrt{3}S=1.5\sqrt{3}$ (right picture). In both figures, the solid line (lower curve) represents the non-propagating computational mode corresponding to the real root, and the dashed line (the upper curve) represents the physical mode corresponding to the principal (complex) root ξ of the characteristic polynomial equation (4.3) that is an approximation to $\exp(i\omega\Delta t)=\exp(ick\Delta t)$. From the Figs. 1 and 2 it can be seen that the modulus of the principal (complex) root is bigger than 1 but $|\xi|=1+\mathcal{O}(\Delta t)$. So the splitting scheme S-FDTD is unconditionally stable and dissipative.

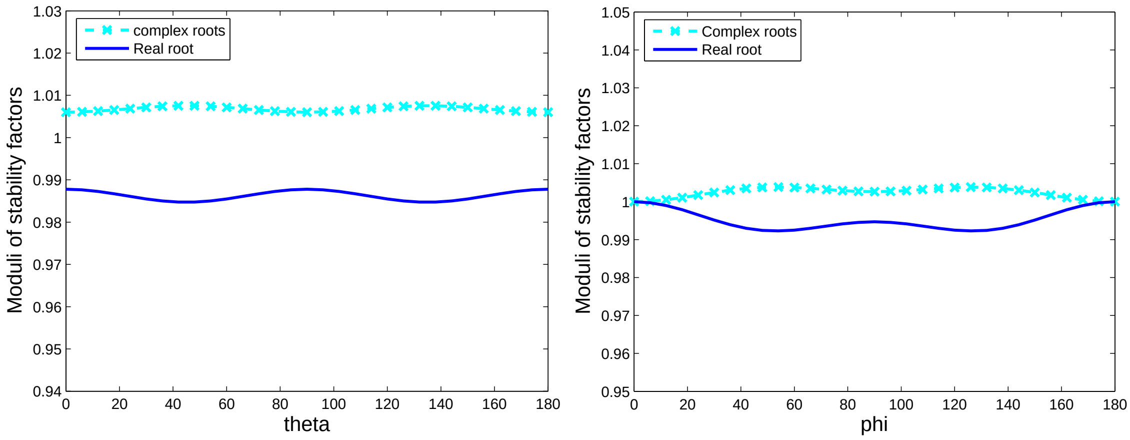

Figure 1: Modulus $|\xi|$ of the three roots of the characteristic polynomial equation (4.3) (or the stability factor) for S-FDTD against the propagation angle θ at a CFL number $\sqrt{3}S=1.5\sqrt{3}$ in the case with $\phi=45^\circ$ and $N_\lambda=30$ (left), and against the angle ϕ at a CFL number $\sqrt{3}S=1.4\sqrt{3}$ in the case with $\theta=35^\circ$ and $N_\lambda=40$ (right).

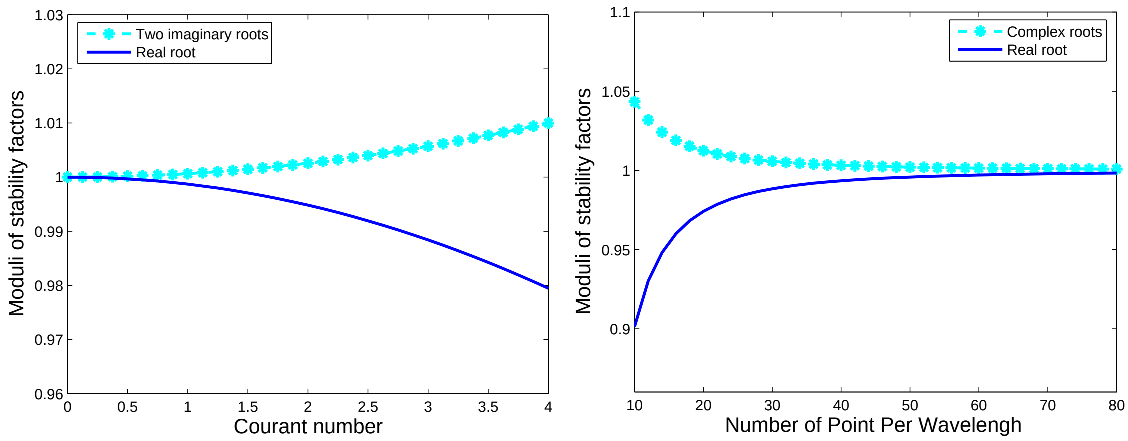

Figure 2: Modulus $|\xi|$ of the three roots of the characteristic polynomial equation (4.3) (or the stability factor) for S-FDTD as a function of S (the CFL number is $\sqrt{3}S$) in the case with $N_\lambda=60$, $\theta=65^\circ$ and $\phi=35^\circ$ (left), and as a function of N_λ (number of points per wavelength) at the CFL number $\sqrt{3}S=1.5\sqrt{3}$ in the case with $\theta=65^\circ$ and $\phi=35^\circ$ (right).

The normalized phase velocity is determined from the principal root ξ as follows (see [25]):

$$
\begin{aligned}
\frac{v_p}{c} &= \frac{1}{\omega\Delta t}\arctan\left(\frac{\Im(\xi)}{\Re(\xi)}\right) \\
&= \frac{1}{ck\Delta t}\arctan\left(\frac{\Im(\xi)}{\Re(\xi)}\right) = \frac{N_\lambda}{2\pi S}\arctan\left(\frac{\Im(\xi)}{\Re(\xi)}\right).
\end{aligned}
\tag{4.4}
$$

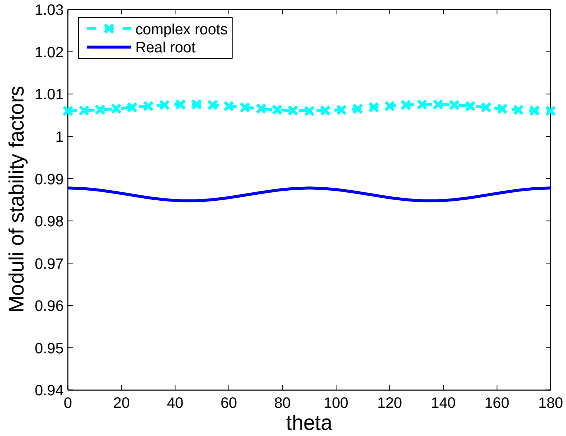

Figure 3: Normalized phase velocity v_p/c as a function of the angle θ at a CFL number of $1.5\sqrt{3}$ in the case with $N_\lambda=20$ (NPPW) and $\phi=40°$ (left) and as a function of the angle ϕ at a CFL number of $3.5\sqrt{3}$ in the case with $N_\lambda=40$ (NPPW) and $\theta=25°$ (right) for S-FDTD and IS-FDTD.

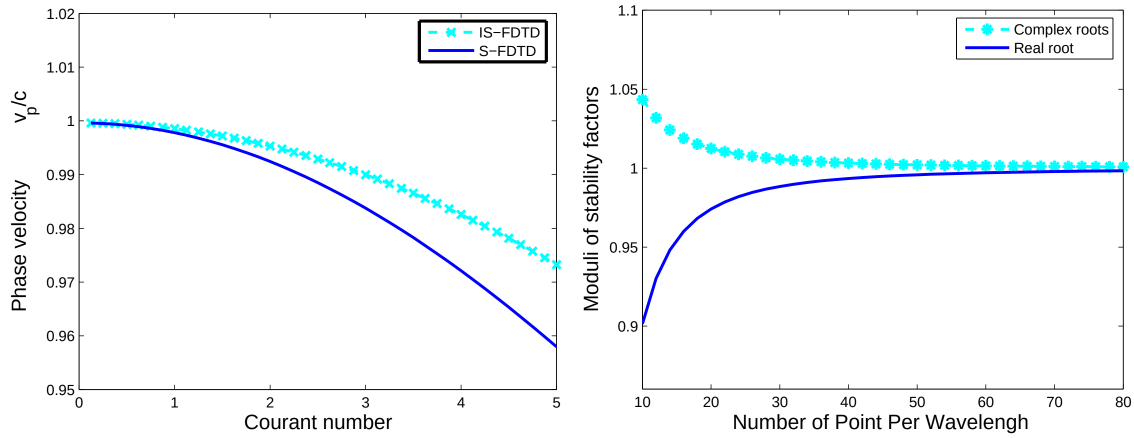

Figure 4: normalized phase velocity v_p/c as a function of S (the CFL number is $\sqrt{3}S$) in the case with $\theta=45°$, $\phi=65°$ and $N_\lambda=40$ (left), and as a function of N_λ (NPPW) at a CFL number of $2.4\sqrt{3}$ in the case with $\theta=35°$ and $\phi=65°$ (right) for S-FDTD and IS-FDTD.

Fig. 3 shows the normalized phase velocity v_p/c as a function of the propagation angle θ at a CFL number of $\sqrt{3}S=1.5\sqrt{3}$ in the case with the number of points per wavelength $N_\lambda=20$ and $\phi=40°$ (left picture) and as a function of the propagation angle ϕ at a CFL number of $\sqrt{3}S=3.5\sqrt{3}$ in the case with the number of points per wavelength $N_\lambda=40$ and $\theta=25°$ (right picture) for the schemes S-FDTD and IS-FDTD. Fig. 4 presents the normalized phase velocity v_p/c as a function of S (the CFL number is $\sqrt{3}S$) in the case with $\theta=45°$, $\phi=65°$ and $N_\lambda=40$ (left picture), and as a function of the number of points per wavelength N_λ at a CFL number of $\sqrt{3}S=2.4\sqrt{3}$ in the case with $\theta=35^\circ$ and $\phi=65^\circ$ (right picture) for the schemes S-FDTD and IS-FDTD. As seen from Figs. 3 and 4, the normalized phase velocity v_p/c of the improved splitting scheme IS-FDTD is much more close to 1 than that of the splitting scheme S-FDTD, which means that the dispersion error of the scheme IS-FDTD is much smaller than that of the scheme S-FDTD.

5 Numerical experiments

In this section we present some numerical results to illustrate the efficiency of the two schemes and verify the theoretical convergence rates of the two schemes in some simple cases. Results obtained by the two schemes are also compared with those given by the ADI-FDTD scheme proposed in [21,27].

In all examples, we assume that $\Omega=[0,1]\times[0,1]\times[0,1]$ and that $\varepsilon=\mu=1$. All the problems were computed using the three schemes: S-FDTD, IS-FDTD and ADI-FDTD and coded in Fortran 77 with implementation in a 1.70GHz PC with 256Mb memory and an operating system Windows 2000.

5.1 Example 1

We firstly assume that $\sigma=\sigma^*=0$. An exact solution of the Maxwell equations (1.1)-(1.6) with the boundary condition (2.1) is:

$$
\begin{aligned}
&E_x=\frac{1}{4}\sqrt{3}\cos(\sqrt{3}\pi t)\cos[\pi(1-x)]\sin[\pi(1-y)]\sin[\pi(1-z)],\\
&E_y=\frac{1}{2}\sqrt{3}\cos(\sqrt{3}\pi t)\sin[\pi(1-x)]\cos[\pi(1-y)]\sin[\pi(1-z)],\\
&E_z=-\frac{3}{4}\sqrt{3}\cos(\sqrt{3}\pi t)\sin[\pi(1-x)]\sin[\pi(1-y)]\cos[\pi(1-z)],\\
&H_x=-\frac{5}{4}\sin(\sqrt{3}\pi t)\sin[\pi(1-x)]\cos[\pi(1-y)]\cos[\pi(1-z)],\\
&H_y=\sin(\sqrt{3}\pi t)\cos[\pi(1-x)]\sin[\pi(1-y)]\cos[\pi(1-z)],\\
&H_z=\frac{1}{4}\sin(\sqrt{3}\pi t)\cos[\pi(1-x)]\cos[\pi(1-y)]\sin[\pi(1-z)].
\end{aligned}
$$

The experiment was carried out with different spatial mesh sizes and CFL numbers. The elapsed CPU time in seconds (CPU) and absolute error of the electric and magnetic fields in the discrete energy norm (E-error, H-error) as well as the estimated rate in time of convergence of **E** and **H** (Rate-E, Rate-H) are provided in Table 1, where the spatial step size is taken as $h=0.01$.

From Table 1 it is seen that the convergence rate in time of S-FDTD is of first-order and that of IS-FDTD and ADI-FDTD is of second-order, as demonstrated by the theoretical analysis. It should be pointed out that the error is dominated by the time discretization

Table 1: Absolute error of **E** and **H** in the energy norm, convergence rate in time and CPU time of S-FDTD, IS-FDTD and ADI-FDTD under different CFL numbers with the spatial step size $h=0.01$ at time $T=1$.

Scheme	Δt	E-error	H-error	Rate-E	Rate-H	CPU
S-FDTD	5h	3.988e-2	6.702e-2			112.1
	4h	3.367e-2	5.139e-2	0.759	1.19	140.1
	2h	1.844e-2	2.345e-2	0.856	1.139	271.66
	1h	9.554e-3	1.120e-2	0.9491	1.067	529.28
	0.5h	4.821e-3	5.498e-3	0.9868	1.026	1192.80
	0.25h	2.387e-3	2.756e-3	1.014	0.9962	2351.69
IS-FDTD	5h	4.831e-3	4.712e-3			147.6
	4h	3.14e-3	3.02e-3	1.93	2.02	182.3
	2h	8.657e-4	7.892e-4	1.859	1.928	355.94
	1h	2.893e-4	2.552e-4	1.581	1.628	703.42
	0.5h	1.441e-4	1.262e-4	1.005	1.016	1398.92
	0.25h	1.078e-4	9.532e-5	0.4298	0.4048	2796.66
	0.125h	9.865e-5	8.783e-5	0.1274	0.1180	5612.53
ADI-FDTD	5h	7.304e-3	6.815e-3			128.0
	4h	4.7e-3	4.405e-3	1.976	1.956	156.6
	2h	1.244e-3	1.167e-3	1.918	1.917	305.02
	1h	3.825e-4	3.533e-4	1.701	1.723	603.42
	0.5h	1.673e-4	1.511e-4	1.193	1.225	1196.01
	0.25h	1.135e-4	1.015e-4	0.5595	0.5736	2401.22
	0.125h	1.001e-4	8.939e-5	0.1818	0.1839	5512.44

error only when $\Delta t \geq h$. Table 1 shows that IS-FDTD is more accurate than ADI-FDTD though IS-FDTD uses about 16.7% more CPU time than ADI-FDTD does. Further, with the CFL number is getting bigger, the scheme IS-FDTD is getting more accurate than the scheme ADI-FDTD.

To see the convergence rate in space of the improved scheme IS-FDTD and the ADI-FDTD scheme we take $h=0.02$ and present the results in Table 2. Table 3 gives the estimated convergence rate in space of the two schemes, which is obtained by using Tables 1 and 2. From Table 3 it is found that the convergence rate in space of the two schemes is of second-order, which is consistent with the theoretical analysis. It should be noted that the error is dominated by the spatial discretization error only when $\Delta t \leq h$. To investigate the performance of the improved splitting scheme IS-FDTD and the ADI-FDTD scheme in a long time, we present Table 4 to show the absolute error and CPU time of the two schemes in the case with $h=0.02$ and time $T=8$. The CFL number is 0.5. From the Tables 1-4 we see that the improved splitting scheme IS-FDTD and the ADI-FDTD scheme are more accurate than the splitting scheme S-FDTD.

Table 2: Absolute error of $\mathbf{E}$ and $\mathbf{H}$ in the energy norm and CPU time of S-FDTD, IS-FDTD and ADI-FDTD under different CFL numbers with the spatial step size $h=0.02$ at time $T=1$.

Scheme	Δt	E-error	H-error	CPU
S-FDTD	2h	3.338e-2	5.165e-2	17.23
	1h	1.816e-2	2.371e-2	32.72
	0.5h	9.278e-3	1.146e-2	64.78
	0.25h	4.549e-3	5.756e-3	129.48
	0.125h	2.119e-3	3.013e-3	258.47
IS-FDTD	2h	3.426e-3	3.236e-3	22.41
	1h	1.152e-3	1.030e-3	43.36
	0.5h	5.759e-4	5.057e-4	87.98
	0.25h	4.310e-4	3.812e-4	167.38
	0.125h	3.947e-4	3.512e-4	386.42
ADI-FDTD	2h	4.988e-3	4.642e-3	18.59
	1h	1.531e-3	1.411e-3	35.95
	0.5h	6.695e-4	6.039e-4	70.81
	0.25h	4.543e-4	4.059e-4	142.02
	0.125h	4.005e-4	3.574e-4	290.47

Table 3: Convergence rate in space of the two schemes IS-FDTA and ADI-FDTD at time $T=1$.

Scheme	Time Step Δt	1h	0.5h	0.25h	0.125h
IS-FDTD	Rate-E	0.993	1.58	1.873	1.967
	Rate-H	0.986	1.595	1.8817	1.969
ADI-FDTD	Rate-E	0.808	1.441	1.819	1.951
	Rate-H	0.773	1.426	1.815	1.950

5.2 Example 2

In this example we assume that $\sigma^*=0$, $\sigma=3\pi^2+1$. The exact solution of the Maxwell equations (1.1)-(1.6) with the boundary condition (2.1) is given by

$$\begin{aligned}
E_x &= \frac{2}{3\pi}e^{-t}\cos(\pi x)\sin(\pi y)\sin(\pi z),\\
E_y &= -\frac{5}{6\pi}e^{-t}\sin(\pi x)\cos(\pi y)\sin(\pi z),\\
E_x &= \frac{1}{6\pi}e^{-t}\sin(\pi x)\sin(\pi y)\cos(\pi z),\\
H_x &= e^{-t}\sin(\pi x)\cos(\pi y)\cos(\pi z),\\
H_y &= \frac{1}{2}e^{-t}\cos(\pi x)\sin(\pi y)\cos(\pi z),\\
H_z &= -\frac{3}{2}e^{-t}\cos(\pi x)\cos(\pi y)\sin(\pi z).
\end{aligned}$$

Table 4: Performance of IS-FDTD and ADI-FDTD at a long time $T=8$ with $h=0.02$.

Scheme	Δt	E-error	H-error	CPU
IS-FDTD	0.5h	2.706e-3	5.558e-3	680.91
ADI-FDTD	0.5h	3.169e-3	6.439e-3	562.42

Table 5: Relative error of $\mathbf{E}$ in the energy norm and CPU time of S-FDTD, IS-FDTD and ADI-FDTD under different CFL numbers with the spatial step size $h=0.01$ at time $T=1$.

Scheme	Δt	RE-E	CPU
S-FDTD	0.5h	2.5228e-2	501.75
	0.4h	2.0317e-2	636.33
	0.25h	1.2828e-2	989.38
	0.20h	1.030e-2	1261.63
IS-FDTD	0.5h	5.5377e-5	707.67
	0.4h	3.8892e-5	889.39
	0.25h	3.3472e-5	1369.44
	0.20h	3.4900e-5	1732.04
ADI-FDTD	0.5h	6.0676e-5	583.69
	0.4h	5.2007e-5	720.01
	0.25h	4.3819e-5	1124.20
	0.20h	4.2184e-5	1401.98

Table 5 presents the relative error of the electric field $\mathbf{E}$ in the energy norm and CPU time of S-FDTD, IS-FDTD and ADI-FDTD under different CFL numbers with the spatial step size $h=0.01$ at time $T=1$. The results show that IS-FDTD is more accurate than ADI-FDTD for this damped wave case.

Acknowledgments

The work of the second author (BZ) was supported by the Chinese Academy of Sciences through the Hundred Talents Program. The work of the third author (DL) was supported by the Natural Sciences and Engineering Research Council, Canada. We thank the referees for their valuable comments and suggestions which greatly helped improve the paper.

References

[1] H. Ammari, H. Kang and E. Kim, Approximate boundary conditions for patch antennas mounted on thin dielectric layers, Commun. Comput. Phys., 1 (2006), 1076-1095.
[2] G. Cohen and M. Durufle, Non spurious spectral-like element methods for Maxwell's equations, J. Comp. Math., 25 (2007), 282-304.

[3] D.B. Davidson, Computational Electromagnetics for RF and Microwave Engineering, Cambridge University Press, 2005.

[4] J.E. Dendy, Jr. and G. Fairweather, Alternating-direction Galerkin methods for parabolic and hyperbolic problems on rectangular polygons, SIAM J. Numer. Anal., 12 (1975), 144-163.

[5] J. Douglas and H. H. Rachford, On the numerical solution of heat conduction problems in two and three space variables, Trans. Amer. Math. Soc., 82 (1956), 421-439.

[6] J. Douglas and T. Dupont, Alternating-direction Galerkin methods on rectangules, in Proc. Sympos. Numer. Solution of Partial Differential Equations II (ed. B. Hubbard), Academic Press, New York, 1971, pp. 133-214.

[7] J. Douglas, Jr. and S. Kim, Improved accuracy for locally one-dimensional methods for parabolic equations, Math. Models Methods Appl. Sci., 11 (2001), 1563-1579.

[8] B. Fornberg, Some numerical techniques for Maxwell's equations in different types of geometries, in Topics in Computational Wave Propagation: Direct and Inverse Problems, Lecture Notes in Computational Science and Engineering 31, Springer-Verlag, 2003, pp. 265-299.

[9] S.G. Garcia, T.W. Lee and S.C. Hagness, On the accuracy of the ADI-FDTD method, IEEE Antennas Wireless Propagat. Letters, 1 (2002), 31-34.

[10] L. Gao, B. Zhang and D. Liang, Analysis of an ADI finite difference method for the time-dependent Maxwell equations in 3-D, in Advances in Scientific Computing and Applications (eds. Y. Lu, W. Sun and T. Tang), Science Press, Beijing/New York, 2004, pp. 171-180.

[11] L. Gao, B. Zhang and D. Liang, The splitting finite-difference time-domain methods for Maxwell's equations in two dimensions, J. Comput. Appl. Math., 205 (2007), 207-230.

[12] S.D. Gedney, G. Liu, J.A. Roden and A. Zhu, Perfectly matched layer media with CFS for an unconditional stable ADI-FDTD method, IEEE Trans. Antennas Propagat., 49 (2001), 1554-1559.

[13] T. Hagstrom and S. Lau, Radiation boundary conditions for Maxwell's equations: A review of accurate time-domain formulations, J. Comp. Math., 25 (2007), 305-336.

[14] T. Huttunen and P. Monk, The use of plane waves to approximate wave propagation in anisotropic media, J. Comp. Math., 25 (2007), 350-367.

[15] J. Huang and A. Wood, Analysis and numerical solution of transient electromagnetic scattering from overfilled cavities, Commun. Comput. Phys., 1 (2006), 1043-1055.

[16] J.A. Kong, Electriomagnetic Wave Theory (2nd Ed.), John Wiley, New York, 1990.

[17] J. Lee and B. Fornberg, Some unconditionally stable time stepping methods for the 3-D Maxwell's equations, J. Comput. Appl. Math., 166 (2004), 497-523.

[18] R. Leis, Initial Boundary Value Problems in Mathematical Physics, John Wiley, New York, 1986.

[19] Y. Lu, Some techniques for computing wave propagation in optical waveguides, Commun. Comput. Phys., 1 (2006), 1056-1075.

[20] P. Monk and E. S*ü*li, A convergence analysis of Yee's scheme on nonuniform grid, SIAM J. Numer. Anal., 31 (1994), 393-412.

[21] T. Namiki, 3-D ADI-FDTD method-Unconditionally stable time-domain Maxwell's equations, IEEE Trans. Microwave Theory Tech., 48 (2000), 1743-1748.

[22] R.A. Nicolaides and D.Q. Wang, Convergence analysis of a covolume scheme for Maxwell's equations in three dimensions, Math. Comput., 67 (1998), 947-963.

[23] D.W. Peaceman and H.H. Rachford, The numerical solution of parabolic and elliptic difference equations, J. Soc. Ind. Appl. Math., 42 (1965), 28-41.

[24] A. Taflove and S. Hagness, Computational Electrodynamics: The Finite-Difference Time-Domain Method (2nd Ed.), Artech House, Boston, MA, 2000.

[25] Z. Xie, B. Zhang and C.H. Chan, An explicit fourth-order staggered finite-difference time-domain method for Maxwell's equaions, J. Comput. Appl. Math., 147 (2002), 75-98.
[26] K.S. Yee, Numerical solution of initial boundary value problems involving Maxwell's equations in isotropic media, IEEE Trans. Antennas Propagat., 14 (1966), 302-307.
[27] F. Zheng, Z. Chen and J. Zhang, Toward the development of a three-dimensional unconditionally stable finite difference time-domain method, IEEE Trans. Microwave Theory Tech., 48 (2000), 1550-1558.
[28] F. Zheng and Z. Chen, Numerical dispersion analysis of the unconditionally stable 3D-ADI-FDTD method, IEEE Trans. Microwave Theory Tech., 49 (2001), 1006-1009.